Sensors and Actuators Reports 4 (2022) 100108

Contents lists available at ScienceDirect

Sensors and Actuators Reports

journal homepage: www.sciencedirect.com/journal/sensors-and-actuators-reports

Copper nanoclusters and their application for innovative fluorescent detection strategies: An overview

Mariagrazia Lettieri, Pasquale Palladino, Simona Scarano, Maria Minunni *

Department of Chemistry "Ugo Schiff", University of Florence, Sesto Fiorentino, FI 50019, Italy

ARTICLE INFO

Keywords:
Copper nanocluster
CuNCs synthetic approach
CuNCs-based assays
Fluorescence detection strategies

ABSTRACT

Nanomaterials have revolutionized the design of the detection strategies, and nowadays nanoparticles are extensively employed in innovative assays for the selective and sensitive detection of a large variety of analytes. Recently, a new nanomaterials category, namely nanoclusters (NCs), is rapidly emerging. These nanostructures offer great advantages in terms of stability and ease of fabrication. The increasing interest in NCs applications, well represented by the wide bibliography reporting on gold and silver NCs, opens new perspectives for copper nanoclusters (CuNCs). Compared to noble metals, CuNCs not only are more easily available and inexpensive, but also display unique photoluminescent properties with large Stokes shifts, low toxicity, and high biocompatibility, providing high sensitivity even in complex biological matrices. In this review, we present some relevant aspects in the application of CuNCs to various detection strategies, reporting the main features that define the most interesting CuNCs properties, focusing on CuNCs as a promising functional nanomaterial for the development of innovative fluorescent-based platforms.

1. Introduction

There is a need in bioanalytical chemistry of simple, easy, sensitive, and inexpensive assays. In the last years, nanomaterials have been used to improve bioassays' analytical performances, mainly in terms of detection limits. Metal or carbon nanostructures have been applied to Surface Plasmon Resonance (SPR) coupled to nucleic acids or protein based biosensing [1,2] or used in fluorescent-based measurements such as quantum dots (QDs). Recently, a new category of nanomaterials, namely nanoclusters (NCs), is rapidly attracting the interest of bio-analytical chemists for the important fluorescence features applied to the development of bioassays.

Metal nanoclusters (MNCs) are exciting and versatile nanomaterials with intermediate properties between isolated metal atoms and metal nanoparticles (MNPs). To date, the majority of the sensing strategies based on MNCs exploit noble metals, *e.g.,* silver (AgNCs) [3] and gold (AuNCs) [4].

Thanks to their low toxicity and high biocompatibility, in the last decade, copper nanoclusters (CuNCs) were successful used in biomedical and biological fields for *in vitro* and *in vivo* applications [5–8], including molecular diagnostics, nanotheranostic, and environmental analysis. Furthermore, copper is less expensive and more accessible on earth than noble metals, positively impacting on NCs-based systems development. CuNCs appear as excellent substitutes of QDs and organic dyes, thanks to high quantum yield (QY), photostability [9], and large Stokes shifts [10]. The outstanding fluorescence and catalysis features of CuNCs are size-dependent [11], limited by definition to few-to-tens atoms, and diameters within 1 nm, leading to a quantum-like behavior with discrete HOMO-LUMO electronic transitions [12].

The first reports on the formation of fluorescent CuNCs nanoclusters were proposed in 1998 by Zaho et al. [13,14]. They used a class of monodisperse polymeric macromolecular compounds (dendrimers) as templates triggering metal ion reduction which stabilize formed metal clusters, avoiding their aggregation [15]. Other useful templates are nucleic acids [16], proteins [17], peptides [18], and small molecules [19], which reduce copper ions and inhibit the formation of aggregates by steric hindrance [20]. CuNCs were used as sensing probes (enhancing or quenching their fluorescence) to achieve the high-sensitive determination of small and macromolecules even in complex real matrices. First studies reported the Pb^{2+} ions detection by using BSA as template for copper clustering and CuNCs fluorescence quenching to reveal Pb^{2+} presence in solution [21]. Since then, CuNCs were used for quali-quantitative molecular targets' analysis [22–26], pH determination [27–30], or biological imaging [31–33]. The coupling of CuNCs

* Corresponding author.
E-mail address: maria.minunni@unifi.it (M. Minunni).

https://doi.org/10.1016/j.snr.2022.100108
Received 23 March 2022; Received in revised form 13 May 2022; Accepted 21 May 2022
Available online 6 June 2022

with a biological recognition element, enabled the development of fluorescence-based platforms characterized by good detection range and detection limit, great stability, and selectivity, which are of great importance in bioanalysis to develop simple and ultrasensitive strategies for biomolecular targets. In this framework, the use of peptides, proteins [34], single (ssDNA), double stranded (dsDNA) [35], and hairpins DNA [36], has been reported [37].

This review firstly describes the general synthetic strategies of CuNCs, then it summarizes the CuNCs-based platform focusing on nucleotides-based CuNCs applied to sensing strategies [38,39] in a framework of easy-to-use, portable, and low-cost devices. Differently from interesting published reviews [38–43], we will distinguish between homogeneous (in solution) and heterogeneous (*e.g.*, lateral flow strips) assays, preserving the definition of sensors and biosensors to devices where a transducer is coupled to a biological receptor immobilized on the surface, including electrodes, planar waveguides, optic fibers, quartz crystals, for electrochemical, optical, and gravimetric based sensing.

2. Synthesis and features of CuNCs

2.1. Experimental parameters that influence fluorescence of CuNCs

The fluorescent properties of CuNCs depend on their nanometric dimensions (Fig. 1) and, similarly to NPs, can be tuned by playing on the synthesis conditions (metal and template concentration/type, reducing agent, solvent, pH, temperature, growth time, etc.), generating atomically precise entities [44]. The emission energy (E_g) of CuNCs depends on Fermi energy of the bulk metal (E_{fermi}) and the number of atoms in single clusters (n), according to equation $E_g=E_{fermi}/n^{1/3}$ [44,45], with the emission wavelengths (λ) spanning from the visible to the near-infrared (NIR) region. Consequently, NCs represent a link between optical properties of a single atom, with discrete electronic transitions between the occupied *d* bands and the Fermi level, and those of nanoparticles, exhibiting localized surface plasmon resonance (LSPR) [46–50]. The core size is directly proportional to the quantity of the reducing agent used during the synthesis but inversely proportional to fluorescence intensity. In particular, fluorescence is limited to NCs with less than ten copper atoms that can be obtained using very low percentages of reducing agent with respect to stoichiometric amount of copper ($\alpha < 0.1$) [51].

Coordination of ligands to the metal core [52] and pH influence both the photoluminescence (PL) of the CuNCs. In particular, electron-rich or electron donor groups, like -SH, –COOH, $-NH_2$ and –OH, increase the emission intensity and fluorescence lifetime of CuNCs [53,54]. Moreover, pH changes lead to CuNCs emission and excitation peaks shifts due to protonation/deprotonation mechanisms [55], inducing aggregation, emission enhancement, and impacting on CuNCs growth [56]. For example, alkaline pH favors disulfide bonds breaking within the protein scaffold, stabilizing CuNCs by thiol groups coordination [57]. Thanks to the CuNCs pH sensibility, pH sensors are reported [58–61] in the range from 2.0 to 13.2.

Solvents also influence CuCNs PL spectra, due to interactions among the ground state, the excited state, and solvent molecules [62,63]. In particular, CuNCs fluorescence spectra show lower number of peaks and greater Stokes shift in solvents with higher polarity [64], but the fluorescent emission intensity is higher when CuNCs are dispersed in solvents with lower polarity [65].

2.2. Synthetic strategies of copper nanoclusters

Top-down and bottom-up approaches are leading strategies to obtain photoluminescent CuNCs (Fig. 2). Top-down synthesis is based on CuNPs resizing to obtain smaller CuNCs; this approach is very laborious [66,67] while the bottom-up one, simple and mostly used, involves the reduction of metal atoms, followed by their aggregation into clusters, often in presence of a stabilizing agent. Different procedures including electrochemical [68], sonochemical [69], photo-reduction [70], microwave-assisted [32], and template-based synthesis [71] are used in the bottom-up approach. In electrochemical methods, an anode is used as the metal ions source that are reduced at the cathodic surface to metal atoms forming aggregates or nanoclusters stabilized by using surfactants [72]. The sonochemical method is a green and easy synthetic method, exploiting ultrasounds derived from acoustic cavitation [73]. Its limitation is the low quantity of metal atoms obtained, which impairs the following nanoclusters' growth. In photo-reduction synthesis, the production of NCs is induced directly by UV radiation [70]. The microwave-assisted method produces rapid CuNCs crystallization due to homogenous and fast heating [72]. The most used approach is the template-assisted one, allowing a facile, fast, cheap, and green synthesis of nanoclusters by using a template to control the kinetics of copper ions reduction, tuning CuCNs size and shape, and preventing their aggregation [74]. Micro and macromolecules like polymers, oligonucleotides, proteins, peptides, and small molecules have been adopted as scaffolds to induce the controlled nucleation of copper nanoclusters as detailed in the following paragraphs.

2.2.1. Nucleotide sequences as templates

Copper ions interact with nucleotide bases through the coordination of the negatively charged phosphodiester backbone [75]. The length and

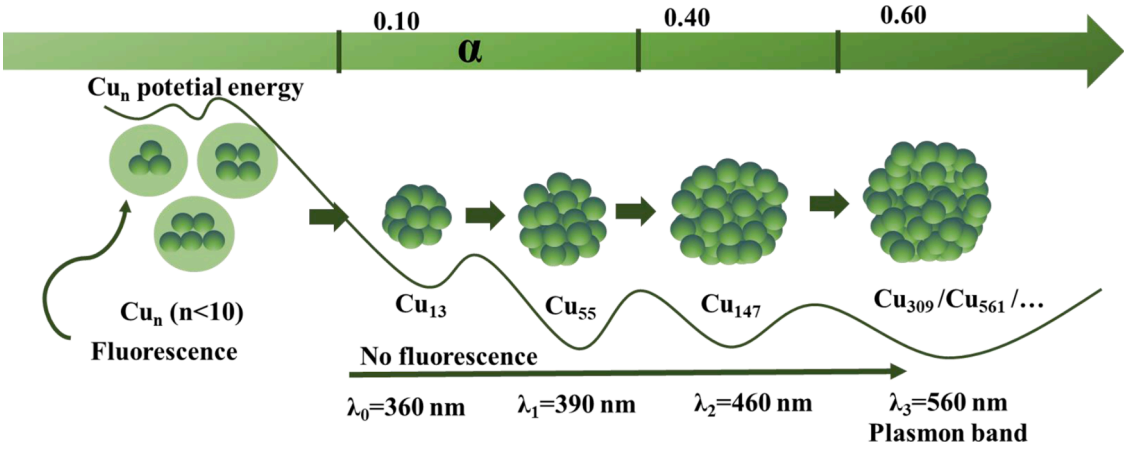

Fig. 1. The influence of the reducing agent-to-copper ratio (α) on CuNCs size (n) and absorption band (λ). Size changes proportionally with α values, whereas photoluminescence is observed when the number of atoms (n) is smaller than 10. The estimated wavelengths (λ) for each cluster and the trend of potential energy are reported [51].

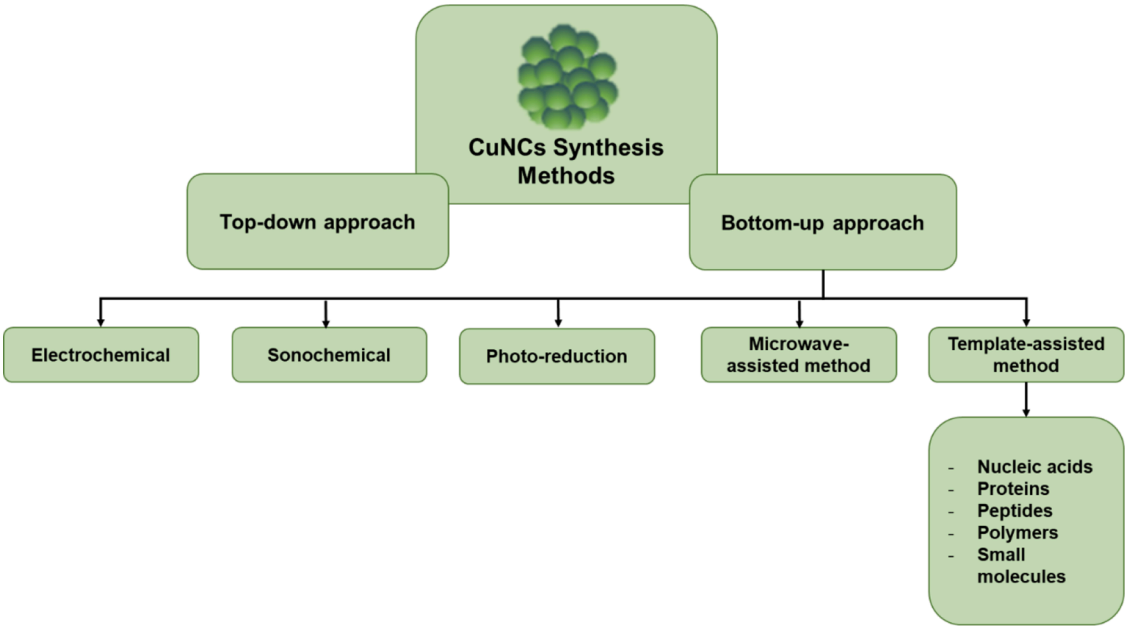

Fig. 2. Synthetic strategies of copper nanoclusters.

the nucleic acid sequence of the dsDNA template strongly influence the CuNCs synthesis and photoluminescence properties [41]. Firstly, random dsDNA was initially exploited for the CuNCs synthesis. Subsequently, it was noticed that a remarkable fluorescent signal improvement was obtained by using polyT ssDNA or poly(AT-TA) dsDNA, where adenine and thymine represent the nucleation site for reduction of Cu(II) to Cu(0) and its clustering to CuNCs. This mechanism is impaired by adopting cytosine and guanine rich sequences likely due to strong copper complexation that could limit copper reduction. Summarizing, ssDNA containing poly(thymine) sequences [76–78], dsDNA with AT-rich domains, as well as long oligonucleotide sequences [79,80], in presence of a reducing agent (usually ascorbic acid), favor the formation of high fluorescent CuNCs with an excitation wavelength at 340 nm and an emission peak around at 600 nm. Beside the stabilizing effect and its influence on the CuNCs photoluminescent properties, nucleotide sequences may also possess specific molecular recognition ability, that can be exploited in solution assays to selectively bind different analytes [81,82], like for the aptamers that are nucleic acid sequences (DNA or RNA) able to bind a target molecule [83,84]. They are obtained *in vitro* after a selection process by exponential enrichment (SELEX) or non-SELEX approaches [85,86]. DNA is a privileged scaffold for the synthesis of CuNCs also because it can be used for a rapid detection of genetic alteration [87], differently from classic genetic tests that usually require long analysis time [88].

2.2.2. *Proteins and peptides as templates*

Proteins and peptides are often used as templates for building stable and biocompatible CuNCs, requiring mild conditions for the synthesis [89,90]. They contain several functional groups, like amine-, thiol- and carboxyl groups, which initiate the complexation through electrostatic forces. Amine- and carboxyl groups coordinate copper ions while thiol groups contribute to the reduction and stabilization of CuNCs. Thus, the diversity of the amino acid sequence affects the final CuNCs properties. A conventional protein-CuNCs synthesis implies the use of various additives that alter the protein structure by breaking the disulfide bonds, like dithiothreitol (DTT) [91], H_2O_2 [92], hydrazine hydrate [93], and NaOH [94]. So far, different protein templates have been explored to synthesize luminescent CuNCs. For instance, bovine serum albumin (BSA) leads to high QY fluorescent CuNCs [81,82,95]. Bustos et al. produced blue emitting CuNCs (610 nm) with high photostability with a decrease of only 15% in emission signal after 50 min [82]. Other proteins, such as human serum albumin (HSA) [96,97], lysozyme [98,99], ovalbumin [100], papain [101,102], transferrin [103] and trypsin [60] have been also applied as templates for CuNCs production. Although proteins are preferred as templates for the presence of multiple active sites that favor the reduction and the accumulation of copper ions promoting the CuNCs growth, few studies report the use of peptides as template [104,105]. For example, Tang and co-workers prepared stable and well water-dispersed CuNCs by reducing copper chloride with ascorbic acid in the presence of a short peptide template Cys-Cys-Cys-Asp-Leu, highlighting the importance of $CuCl_2$-to-peptide molar ratio (1:4) in the formation of CuNCs [104].

2.2.3. *Polymers as templates*

Dendrimers, *i.e.*, highly ordered branched polymers with different size and the chemical structure, are the most exploited templates to produce very stable CuNCs [13,106]. Polyvinyl pyrrolidone (PVP)-CuNCs were applied to develop a FRET-based assay in solution (named sensor) for the micromolar detection of glutathione (GSH) in human serum with performances comparable to HPLC [107]. Polyethyleneimine (PEI) was also used as scaffold for facile one-pot synthesis of water soluble CuNCs applied to Fe^{2+} detection in tap, river water, and urine, with very good analytical performances, *i.e.*, micromolar level concentration and 100% recovery [108]. Furthemore, CuNCs were incorporated into composite polymer films by reduction of copper ions in a hydrogel network with 30% QY, opening to possible applications in heterogeneous phase assays/sensors [109].

2.2.4. *Small molecules as templates*

Small molecules, containing thiolates and carboxylates groups, like glutathione (GSH) and cysteine, act as reducing, protecting, and capping agents to stabilize CuNCs through to a facile one-step green synthetic approach [110–114]. Glutathione was exploited also for its ability to coordinate metal cations like aluminum ions that guide the self-assembly of nanoclusters resulting in the formation of CuNCs with controllable size and retained bright luminescence in neutral conditions [115,116]. Many authors took advantage of the easy and cheap synthesis of copper nanoclusters by using small molecules as template [117–120]. Additional small molecules like 4-methylthiophenol and 4-chlorothiophenol were also applied to synthesize CuNCs able to

sensitively detect different kinds of target molecules like tetracycline (LOD 40 nM) [121].

3. CuNCs-based detection strategies

CuNCs were exploited as sensing probes in solution since they are able to detect different types of targets, from ions to macromolecules (*i.e.*, proteins, DNA, enzyme, etc.) [122]. Numerous publications are related to the integration of noble metal nanomaterials in bioanalytical assays development [123–126], leading to remarkable improvement in bio-detection processes.

Generally, an efficient detection system should be characterized by the following properties: stability, selectivity towards the analyte, reproducibility, desired sensitivity, a null or minimal sample pre-treatment. Moreover, to ensure the development of a potential commercial device, the assay should be simple, cheap, and able to perform rapid analysis making it suitable as a point-of-care (POC) test [127–129].

Copper nanoclusters employed as signal transducers in "sensors" design lead great advantages in the assay performance, such as high selectivity, sensitivity, low detection limits, and wide detection range. Typically, when the bioreceptor is associated with CuNCs, the binding event leads to a fluorescence signal variation depending on analyte concentration [130–132].

In the following sections, different types of detection strategies combined with CuNCs are reported, with the focus on oligonucleotide sequences as bioreceptors both in solution and in heterogeneous assays. Nucleic acids are employed for CuNCs growth and may hybridize or not the complementary DNA sequences. Alternatively, NAs act as synthetic biomimetic receptors *i.e.*, aptamers, binding different analytes (both small and macromolecules), leading to several detecting strategies. The nucleic acids-, proteins-, and immuno-based approaches will be

Table 1
DNA-based detection strategies for CuNCs-based assays.

Template	Target	Technique	Read out	Sample	Linear range	LOD	QY	Refs.
dsDNA	miRNAs	*340/608 nm	Turn-on	-	1.0 pM–10.0 nM	1 pm	-	[134]
polyT DNA	miRNA21	*340/605 nm	Turn-on	Cancer cells	50 pM – 1 nM	18.7 pM	-	[135]
hp-DNA	miRNA155	*400/510	Turn-on	Human serum, saliva, plasma, MCF-7, fibroblast	5.0 pM −10.0 nM	2.2 pM	-	[136]
AT-rich dsDNA	miRNAs	*340/580 nm	Turn-on	Urine	-	500 fM	-	[137]
dsDNA	T4 PNKP	*340/570 nm	Turn-off	HeLa cells	0.07–15.0 U mL	60 U L	3.4 %	[155]
AT-rich dsDNA	MNase	*340/570 nm	Turn-off	-	1.0–50 U L	1.0 U L	-	[142]
dsDNA	ExoIII	*345/610 nm	Turn-off	-	-	-	-	[168]
hpDNA	S1 nuclease	*490/660 nm	Turn-on	-	5.0–8.0 U L	3.0 U L	-	[36]
AT-rich dsDNA	EcoRI	*340/575 nm	Turn-off	-	2.0 −100 U mL	0.87 U mL	-	[79]
polyT DNA	UDG	*345/650 nm	Turn-on	HeLa Cells	0.05–2.0 U L^{-1}	0.002 U L^{-1}	-	[143]
polyT DNA	UDG	*340/602 nm	Turn-on	HeLa Cells	0.1–10 U L	0.05 U L^{-1}	-	[144]
AT-rich dsDNA	UDG	*340/570 nm	Turn-off	HeLa Cells	1.0 – 100 U L	0.5 U L^{-1}	0.039	[145]
AT-rich dsDNA	Dam MTase	*340/590 nm	Turn-off	Human Serum	0.5–10.0 U mL	0.5 U mL	-	[146]
AT-rich dsDNA	TdT	*340/570 nm	Turn-on	Leukemia cells	0.7–14.0 U mL	60.0 mU L^{-1}	0.112	[147]
dsDNA	SNP	*344/593 nm	Turn-on	-	-	-	-	[138]
polyT DNA	SMN1	*340/500 nm	Turn-on	Clinical samples	-	-	-	[139]
dsDNA	Abasic sites	*340/585 nm	Turn-off	Linear plasmid, onion and HeLa Cells	-	-	-	[140]
Nucleosides	Nucleosides	*300/380 nm	Turn-on	-	-	-	0.27–1.34%	[141]
Nanowire-DNA	TdT and BamH1	Electrochemical	Turn-on	Human serum and urine	0.5 −160 U mL^{-1} (TdT); 2×10^{-2} −30 U mL^{-1} (BamH1)	100 U L^{-1} (TdT); 4 U L^{-1} (BamH1)	-	[156]
AT-rich dsDNA	miRNA21	ECL	Turn-on	Human breast cancer cells (MCF-7) and human cervical cancer cells (Hela)	100 aM–100 pM	16.05 aM	-	[157]
AT-rich dsDNA	miRNA155	ECL	Turn-on	Human serum	100 aM– 100 pM	36aM	-	[158]
polyT-DNA	miRNA155	Colorimetric	Turn-off	Human plasma	1.0 pM to 10.0 nM	0.6 pM	-	[159]
dsDNA	HBV DNA	Colorimetric	Turn-on	Human serum	12×10^{9}–12×10^{13} DNA molecules	12×10^{9} DNA molecules	-	[160]
polyT-DNA	DNA	SPR	Turn-on	-	-	3.21 fM	-	[163]

* Fluorescence ($\lambda_{ex}/\lambda_{em}$)

discussed with the focus in real matrices detection, when available in the literature.

The CuNCs-based solution assays/sensors are reported in three tables and three paragraphs to differentiate DNA- (Table 1, paragraph 3.1), aptamer- (Table 2, paragraph 3.3), and immuno-based (Table 3, paragraph 3.3) detection strategies, *i.e.*, defining the probe used for the biorecognition of the target molecule. Within each table and detection strategy, the assays are classified according to the template used for copper reduction and CuCNs generation, the target molecule, the analytical technique used for signal transduction, the turn-on/turn-off read out, the kind of sample, and the analytical parameters, *i.e.*, the linear range for the detection of the analyte, the limit of detection (LOD), and the QY for fluorescent probes only.

3.1. DNA-based detection strategies

3.1.1. Fluorescent detection of oligonucleotides

One of the most used biorecognition elements in sensing strategies are nucleic acids, in particular, single stranded DNA [133]. In the case of CuNCs, DNA sequences have a dual role. They act as template and molecular probe at the same time, stabilizing NCs and selectively binding the analyte. The recognition mechanism involves affinity interaction, hybridization between the probe and complementary sequences or, as in the case of aptamers, Van der Waals, hydrogen bonding, and electrostatic interactions, without hybridization. The crucial role of miRNAs in the regulation of gene expression and, consequently, their association with several diseases, prompted the development of CuNCs-based assays. The pioneering work from Ye's group reported the miRNA detection via an isothermal enzymatic reaction [134], using an amplified template to generate a dsDNA as scaffold for the synthesis of fluorescent CuNCs, showing a detection range from 1 pM to 10 nM (Fig. 3A). Subsequently, similar assays were proposed [134–137]. In particular, miRNA21 was determined in cancer cells by using a duplex-specific nuclease (DSN). When miRNA binds the DNA probe, the DSN digests the DNA sequence, releasing an oligonucleotide that forms a long polyT acting as scaffold for the synthesis of high fluorescent CuNCs [135] (Fig. 3B). DNA-CuNCs are also employed to identify single nucleotide polymorphisms (SNPs) [138], or nucleotide variants [139–141], linked to diseases and drug responses. For example, Chen and coworkers [139] used luminescent polyT (DNA)-CuNCs to identify the Survival Motor Neuron genes SMN1 involved in spinal muscular atrophy, observing fluorescence in 65 DNA clinical samples containing the SMN1 gene. This approach could be exported to other SNPs or nucleotide variants by designing suitable sensing probes (Fig. 3C).

3.1.2. Fluorescent detection of enzymes and small molecules

DNA-CuNCs based assays are also applied to detect enzymes and their activity. Recently, Zhang and coworkers designed a fluorimetric method to detect the activity of the T4 polynucleotide kinase phosphatase (PNKP) by using a short phosphorylated DNA (pDNA) strand, and a long-dephosphorylated DNA (dsDNA) as complementary probes [119]. When PNKP is present, pDNA undergoes dephosphorylation and the dsDNA thus operates as template for CuNCs growth (Fig. 3D). Several research groups adopted similar strategies to develop different DNA-based bioassays for micrococcal nuclease [142], exonuclease III [141], S1 nuclease [36], endonuclease EcoRI [79], Uracil-DNA Glycosylase (UDG) [143–145] and transferase [146,147]. Details relative to LODs and detection ranges of the cited assays are reported in Table 1.

Finally, DNA is also employed as an indirect probe to detect ions [80, 148], or small molecules [149–154]. In these cases, the fluorescent signal could be the result of:

- Interaction between copper ions and small molecules;
- Electron transfer effect between copper ions and the detected target;
- Oxidation of CuNCs;
- Binding between the small molecule and the DNA template, resulting in CuNCs formation;
- Binding between the small molecule and the DNA template which leads to DNA destruction, avoiding CuNCs growth.

3.1.3. Electrochemical and electro-chemiluminescence detection strategies

Most CuNCs-based detection strategies exploit their PL properties for direct analyte detection. However, alternative analytical electrochemical and electrochemiluminescent (ECL) methods have been proposed [156–160] also because of low fabrication costs, simple and low-cost experimental setup, as well as high sensitivity and selectivity. ECL is a kind of luminescence produced by an electrochemically generated intermediates, and the absence of a light source dramatically reduces the background signal from scattered light and luminescent impurities [161]. In this context, Hu et al. reported a CuNCs DNA-based electrochemical sensor to determine the enzymatic activity of terminal deoxynucleotidyl transferase (TdT) that catalyzes the growth of long T-rich DNA nanowires, here used as CuNCs template, further attached to a graphene oxide (GO)-modified electrode where occurs the H_2O_2 reduction, with an electrochemical signal proportional to the TdT amount (LOD = 0.1 U mL^{-1}, detection range: 0.5–160 U mL^{-1}) [156]. The same strategy has been applied to test BamH1 activity, an site-specific endonuclease employed to detect hepatitis C virus (LOD = 0.004 U mL^{-1}, detection range: 0.02–30 U mL^{-1} [156]).

Different sensing mechanisms based on ECL were designed [157, 158]. For example, miRNA21 was detected within an excellent concetration range 100 aM - 100 pM, with the ultrasensitive detection limit of 19 aM [157]. The same range and a LOD of 36 aM was obtained for microRNA-155 detection by using an innovative DNA probe (DNA nanocranes) stabilized by an AT-rich domain [158] (Fig. 4A).

3.1.4. Colorimetric detection strategies

Simple colorimetric assays for NA detection are also reported,

Table 2
Aptamer-based detection strategies for CuNCs-based assays.

Template	Target	Technique	Read out	Sample	Linear range	LOD	QY	Refs.
DNA	ATP and ADA	*460/580 nm	Turn-on (ATP), Turn-off (ADA)	Fetal bovine serum	2–18 mM (ATP); 5–50 U L^{-1} (ADA)	7.0 μM (ATP); 5 U L^{-1} (ADA)	-	[170]
dsDNA	MC-LR	*34/575 nm	Turn-off	Water	0.01–1000 mg L^{-1}	4.8 ng L^{-1}	-	[174]
polyT-DNA	VEGF165	*332/393 *463/524 nm	Turn-on	Human serum	10–800 pM	12 pM	0.082	[175]
PDANS	PKA	*390/492 nm	Turn-off	HepG2 cell lysates	0.05–4.5 U mL^{-1}	0.021 U mL^{-1}	1.24%	[172]
dsDNA	PKA	*345/595 nm	Turn-off	HepG2 cell lysates	0.1–5.0 U mL^{-1}	0.039 U mL^{-1}.	-	[177]
dsDNA	ATP	*340/598 nm	Turn-on	-	0.01 nM - 100 nM	5 pM	-	[171]
Y-DNA	miRNA21	Electrochemical	Turn-on	Human blood	0 pM-0.1fM	10 aM	-	[176]

* Fluorescence ($\lambda_{ex}/\lambda_{em}$).

Table 3
Immunoassay-based detection strategies for CuNCs-based assays.

Template	Target	Technique	Read out	Sample	Linear range	LOD	QY		Refs.
-	HIV-1 p24	*394/598 nm	Turn-on	Human plasma	27–1000 ng L^{-1}		23.8 ng L^{-1}	-	[178]
BSA	PKA	Electrochemical	Turn-on	Human serum	0.5 ng L- 100 ug L		146 pg L	-	[179]
-	LSR	PEC-Colorimetric	Turn-off	Human serum	1 pg L^{-1}–10 ug L^{-1}		1 pg L^{-1}	-	[180]
dsDNA	ALP	*340/575 nm	Turn-on	Human serum	0.04–100 U L^{-1}		7.0 ng L^{-1}	-	[181]
DNA	PSA	PEC	Turn-off	Human serum	0.02–100 ug L^{-1}		5.0 ng L^{-1}	-	[182]
DNA	MM-7	Potentiometric	Turn-on	Human serum	0.02–100 ug L^{-1}		5.3 ng L^{-1}	-	[184]
-	hc-TnT	PEC	Turn-off	Human serum	0.1 to 2 ng L		0.03 ng L	-	[183]

* Fluorescence ($\lambda_{ex}/\lambda_{em}$).

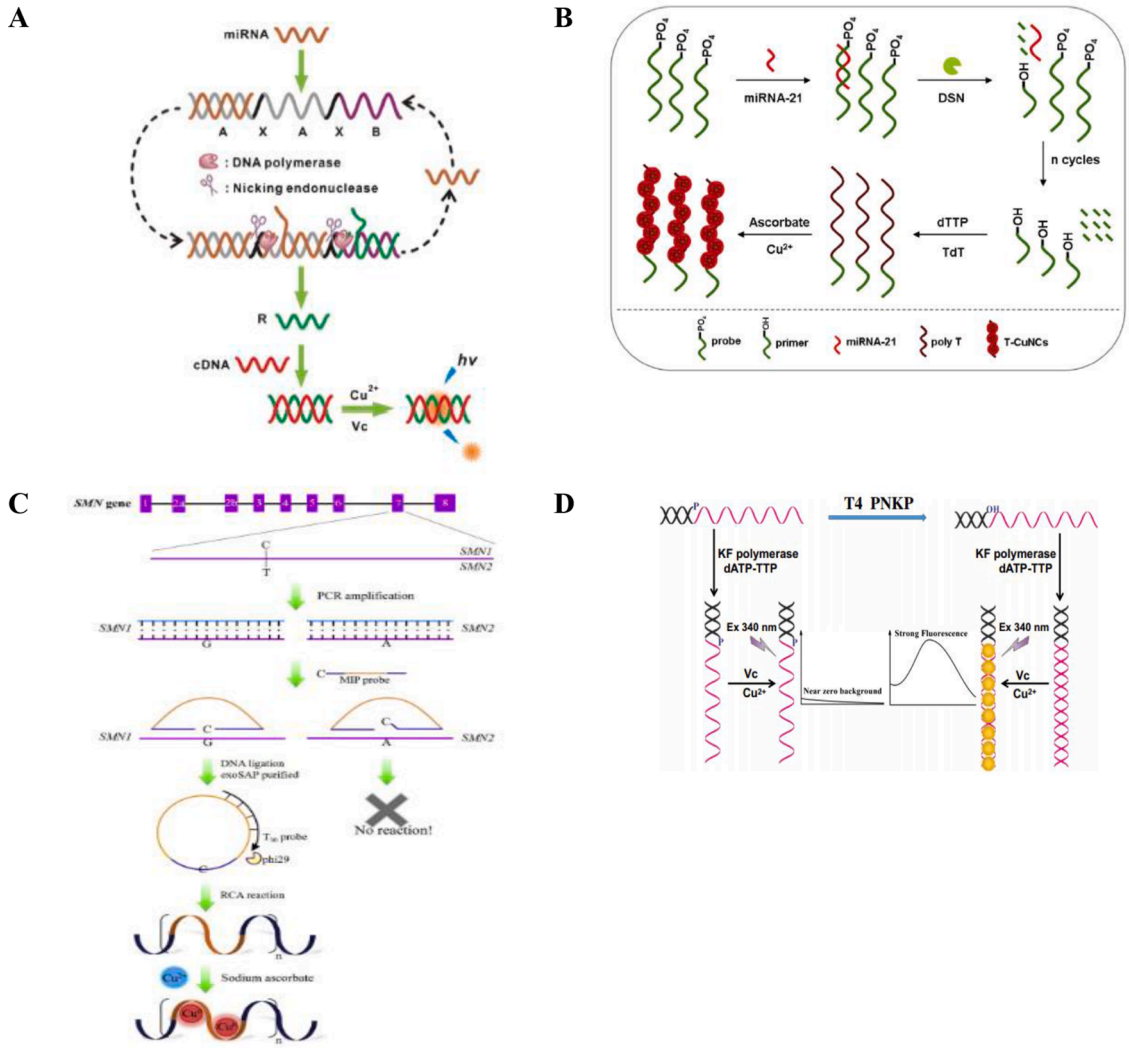

Fig. 3. Schematic illustration of CuNCs DNA-based assays for: (A) miRNA detection according to the assay strategy proposed by Ye's group, reprinted from Ref. [134] with permission of Royal Society of Chemistry; (B) miRNA detection according to the assay strategy proposed by Li's group, reprinted from Ref. [135] with permission of Elsevier B.V.; (C) enzymes detection according to the assay strategy proposed by Zhang and co-workers, reprinted from Ref. [155] with permission of Springer Nature; (D) nucleotide variants detection according to the assay strategy proposed by Chen and co-workers, reprinted from Ref. [139] with permission of Elsevier B.V.

employing CuNCs DNA platforms [91,160,162,163]. Borghei and co-workers developed a colorimetric assay based on methylene blue (MB) to detect a cancer biomarker miRNA-155 in solution. In detail, polyT-DNA was used for CuNCs synthesis, exhibiting an enzyme-like peroxidase activity (Fig. 4B). After miRNA-155 incubation, the complementary sequence on DNA-CuNCs hybridizes miRNA sequences and CuNCs catalyze the oxidation of the methylene blue [159]. Increasing the miRNA concentration, the absorbance of MB decreases with a dynamic range from 1.0 pM to 10.0 nM with a LOD equal to 0.6 pM. Application to the detection in human blood plasma resulted in excellent recovery (99%). This offers an interesting application in clinical diagnostics since miRNA-155 amount can be related to cancer stage and expression, increasing with advancing cancer stage. The use of MB is not new in DNA sensing, since it has been widely and successfully reported coupled to electrochemical transduction [164], but reinforces the CuNCs applicability to companion diagnostics.

Virus detection has also been successfully achieved by an inexpensive colorimetric heterogeneous assay to identify Hepatitis B virus

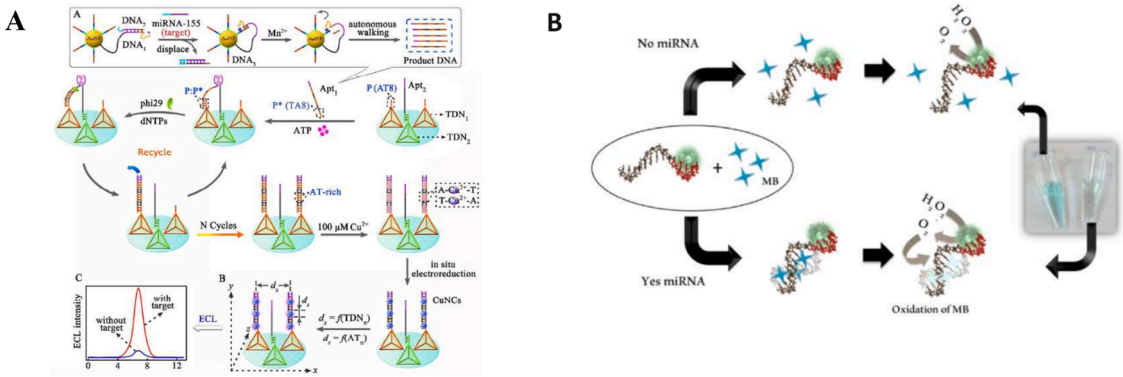

Fig. 4. Schematic illustration of CuNCs DNA-based (A) electrochemiluminescence (ECL) platform according to the assay strategy proposed by Zhou et al. reprinted from Ref. [158] with permission of American Chemical Society (C) colorimetric platform according to the assay strategy proposed by Borghei et al. reprinted from Ref. [159] with permission of Elsevier B.V.

(HBV) by naked eye [160], with possible use in remote areas. In this strategy, a ssDNA probe is immobilized on the surface of a 96-well plate, hybridizing the complementary HBV NA, if present. The resulting dsDNA acts as a CuNCs template. To reveal the hybridization by naked eye, a chromogen is necessary. Thus, simple and cheap reagents leading to ox-red reactions, with final color development, are further added to the mixture:

(1) creatinine with the consequent formation of a copper-creatinine complex
(2) Azino-bis(3-ethylbenzothiazoline-6-sulfonic acid) diammonium salt (ABTS used as substrate)
(3) H_2O_2

The copper-creatinine complex shows peroxidase-like enzyme properties converting H_2O_2 into H_2O and ABTS into its oxidized form [160]. Different concentrations of HBV DNA led to different degrees of ABTS oxidation reaction and, consequently, different green color gradations. This assay was applied also to explore single nucleotide polymorphism (SNP) analysis, in which, in case of SNP presence, decreased color intensity *versus* wild type DNA, can be observed. The possibility to analyze the presence of the target sequence, wild type or mismatched (SNP), in the sample by naked eye and using very simple chemistry, represents an important possibility for bioanalytical applications *in situ*, in remote and/or disadvantaged places of the planet.

3.1.5. Surface Plasmon resonance (SPR)

SPR spectroscopy was explored in combination with CuCNs [163] to achieve ultrasensitive NA detection in real samples [165–167] (*i.e.*, human blood), including SNP detection. An interesting approach is reported by Yuan et al. dealing with the CuCNs synthesis on dsDNA formed at the SPR gold chip surface, followed by target NA extension by terminal deoxynucleotidyl transferase. Here, TdT-mediated prolongation reaction was activated onto the dsDNA modified gold chip, originating an origami scaffold for CuCNs synthesis and precipitation by addition of ascorbic acid, leading to an ultrasensitive determination of femtomolar-level nucleic acid [163].

3.2. Aptamer-based detection strategies

3.2.1. Fluorescence detection

Another important class of oligonucleotide-based sensing strategy exploits aptamers as a biorecognition element, where the aptamers are short ssDNA or ssRNA sequences able to recognize a specific target [169]. The aptamer-target recognition is independent from both the detection principle and signal transduction that can be optical (*e.g.*, fluorometric, colorimetric, plasmonic, etc.), electrochemical, or piezoelectric. Conventional fluorescent aptamer-based platforms (not employing CuNCs) use a fluorophore and a quencher label to produce a Förster resonance energy transfer (FRET) event in which a fluorophore (the donor), in an excited state, transfers its energy to a neighboring molecule (the acceptor) by nonradiative dipole-dipole interaction. Although not necessary, in most cases the acceptor is also a fluorescent dye. In biological applications, this technique has become popular to qualitatively map protein-protein interactions.

In aptamer-based assays, the presence of the target triggers a change in the aptamer conformation, corresponding to a distancing between fluorophore and quencher and, in turn, a fluorescent response. FRET technique has been extensively investigated, however presents some limitations such as low fluorescent signal, due to an overlap between donor emission and acceptor excitation spectra, leading to low quantum yield and low sensitivity, high background due to an incomplete quenching phenomenon, and high cost of the labeled aptamer. These drawbacks encourage the design of new aptamer-based platforms, where CuNCs are exploited as fluorescent probes and the DNA aptamer acts both as template and bioreceptor. Currently, Zhang and Wei developed a 'turn-on' fluorescent method based on DNA-templated copper/silver nanoclusters (DNA-Cu/Ag NCs) for the detection of ATP (adenosine triphosphate) and the enzyme ADA (adenosine deaminase) [170], involved in the purine metabolism, playing a central role in the differentiation and maturation of the lymphoid system. The aptamer sequence is inserted in the middle of the DNA template (Fig. 5A). When the aptamer binds ATP or ADA, it changes its conformation, and, consequently, DNA-Cu/Ag NCs get closer, becoming bright emitters. This approach, in standard solutions, showed a linear range of 2–18 mM and of 5 to 50 U L^{-1} with 7.0 μM and 5 U L^{-1}as LOD, respectively for ATP and ADA. Furthermore, the approach succeeded also in detecting ATP and ADA in a complex matrix, *i.e.*, fetal bovine serum, opening new perspective for a real applicability of this strategy. This aptamer-based "turn-on" fluorescent assay combined with Cu and Ag and nanoclusters is the only example found so far, including silver.

ATP detection has been achieved also by a fluorescent aptasensor, where the structural switch induced by the affinity ATP binding leads to the aptamer harpin open conformation. This results in a primer hybridization which drives a target-cycling strand displacement amplification (TCSDA). As a result, a large quantity of dsDNA is produced, acting as template for CuNCs growth with high fluorescent signal [171]. Relatively to enzymatic activity testing a FRET-based assay for Protein Kinase (PKA) is also reported. In this case, an aptamer-based "in solution" assay/sensor utilizing CuNCs and polydopamine nanospheres (PDANS) was employed [172]. The ATP- CuNCs aptamer (apt-CuNCs) was adsorbed onto PDANS surface. The ox/red event regulates the signal generation. Here the donor apt-CuNCs is in close proximity to the acceptor polydopamine (PDANS), leading to apt-CuNCs fluorescence

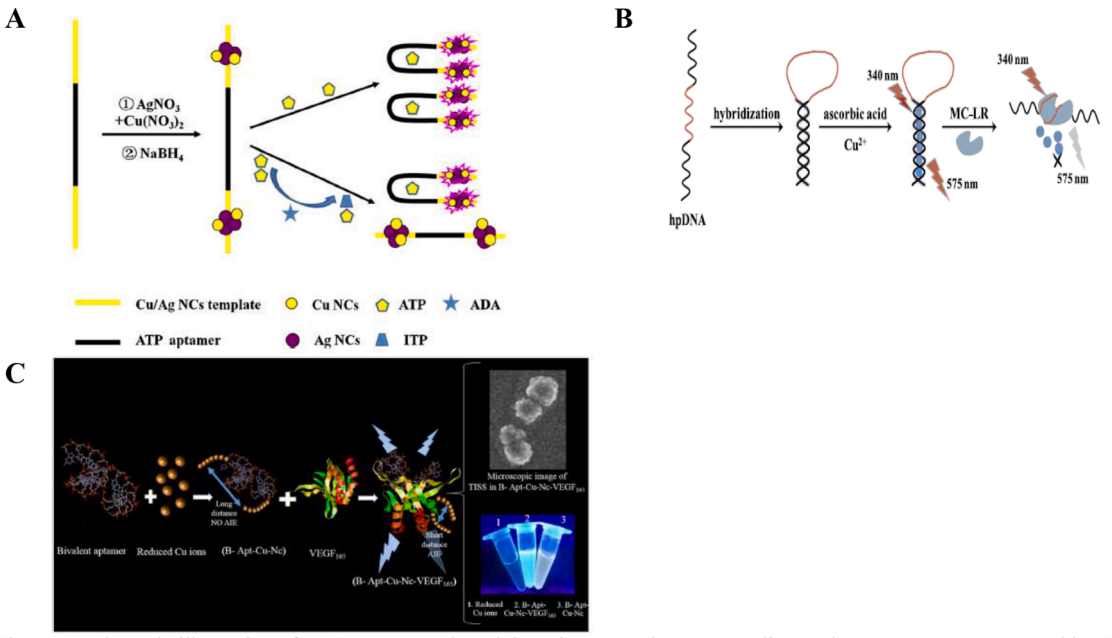

Fig. 5. Schematic illustration of CuNCs-aptamer based detection strategies (A) according to the assay strategy proposed by Zhang and Wei, reprinted from Ref. [170] with permission of Springer Nature. (B) according to the assay strategy proposed by Yanli Zhang's group, reprinted from Ref. [174] with permission of Elsevier B.V. (C) according to the assay strategy proposed by Moghadam's group, reprinted from Ref. [175] with permission of Elsevier B.V.

quenching.

In the case of toxic molecules analysis, an assay targeting microcystins is reported. Microcystins are toxins produced by cyanobacteria with microcystin-leucine arginine (MC-LR) [173]. Zhang et al. designed an aptamer-CuCNs assay selective for MC-LR. The aptamer is also designed to hybridize the complementary DNA sequence (cDNA) which acts as template for CuCNs growth (dsDNA-CuNCs) (Fig. 5B) [174]. After MC-LR addition, the affinity interaction aptamer-target leads to aptamer conformational changes resulting in DNA hybrid (dsDNA/-CuNCs) opening, with CuCNs fluorescence quenching. MC-LR detection in 0.01 to 1000 mg L^{-1} concentration level, with 4.8 ng L^{-1} as LOD in real water samples is reported.

Relatively to protein detection, Vascular Endothelial Growth Factor (VEGF) was quantified via a "signal-on" fluorescent method, based on bivalent aptamer-CuNCs (Fig. 5C) [165]. A multimerized VEGF aptamer works as template for CuCNs growth. VEGF detection is successfully achieved in the 10–800 pM linear range with a LOD of 12 pM. The selectivity and specificity assessment displayed high discriminant capability in serum samples. This strategy is based on a previous work conducted by the same research group, in which graphene dioxide and dsDNA were employed [167].

3.2.2. *Electrochemical detection*

miRNA21 detection has been reported also with electrochemical techniques [176]. Here NA sequences are immobilized on a gold electrode (GE), and the analysis is performed by differential pulse stripping voltammetry (DPSV) [176], by detecting the Cu^{2+} ion of dissolved and stripped CuNCs. miRNA21, as already underlined, is a very interesting

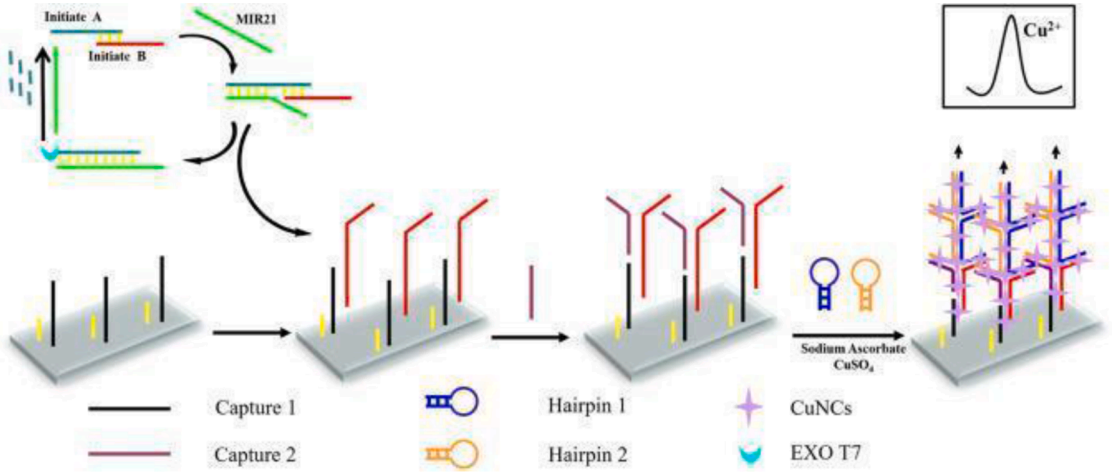

Fig. 6. Schematic illustration of CuNCs aptamer-based electrochemical platform according to the assay strategy proposed by Yijia Wang's research group. This reported detection strategy consists in a multi-steps assay. First, sequence A and B are mixed together to form a duplex DNA. Thus, in this first step A and B are hybridized. Then, it was added MIR21 that lead a displacement between A and B. At this point, EXO T7 degrades A and the fragment binds MIR21 forming a hybrid sequence. Instead, sequence B contributes to the Y-shaped DNA with capture 1 and capture 2 on the electrode. Once obtained the final arrangement of the detection strategy, the Y-shaped branched DNA was used as template for CuNCs synthesis to finally detect MIR21 through oxidation peak current of copper by using DPSV techniques. From Ref. [176], with permission of Elsevier B.V.

target, upregulated in many pathological conditions including cancer and cardiovascular diseases. The approach proposes the fast (in 3 min) and precise *in situ* growth of CuNCs on tree-like overlapping and branching Y shaped dsDNA on the electrode surface [176], with the advantage of being time-saving and allowing controlled dimension of CuNCs (with diameter around 2.5 nm). A simplified scheme is reported in Fig. 6. The assay results a bit cumbersome, requiring several experimental steps: immobilization of NA probes, efficient enzyme with nuclease activity (exonuclease T7 for triggered targets recycling) to cleave only one strand of dsDNA, and the hybridization chain reaction (HCR) amplification for more signal molecules loading on Y-shaped dsDNA [176]. To obtain the Y-shaped branching DNA template, aptamers and hairpin sequences are adsorbed on the gold electrode surface. Subsequently, miRNA21 is added to form the overlapping Y-shaped branching ds-DNA template. This latter was exploited as a template to grow CuNCs. Then, the electrode was immersed in a HNO_3 solution which oxidized Cu (0) to Cu (II) that is thus released in solution. In conclusion, miRNA21 is determined by the oxidation peak current of copper obtained by applying differential pulse stripping voltammetry (DPSV) analysis. The aptasensor shows a linear range within 10 pM and 0.1 fM and 10 aM as LOD. This LOD is competitive with the ones recorded with fluorescence and ECL detection respectively in the order of pM [135] and aM [157] as displayed in Table 1. Moreover, this electrochemical platform was tested in blood samples, with around 100% recovery in human blood spiked with miRNA21 down to 0.1 fM, demonstrating an excellent ability to operate in real samples.

3.3. Immuno-based CuNCs assays

Over the past decades, considerable advances have interested the design of immunoassays thanks to the introduction of photoluminescent metal nanomaterials that improved the detection efficiency of biomolecules. However, the combination of CuNCs with immuno-based strategies is still poorly applied and only few studies are reported in the literature. Among these, detection strategies involving the growth of CuNCs on glutathione (GSH) and the subsequent coupling to streptavidin have been reported for detection of HIV-1 p24 biomarker in AIDS tests [178]. In particular, a secondary biotinylated antibody interacts with a CuNCs-conjugate streptavidin, emitting a fluorescence signal HIV-1 p24 concentration dependent (Fig. 7A). A dynamic range of 27–1000 pg mL^{-1} is achieved with a LOD of 23.8 pg mL^{-1} standard solution. Reliable results were obtained also in plasma samples spiked with known concentrations of p24 antigen. Moving to tumor markers analysis, prostate specific antigen (PSA) detection was achieved by electrochemical detection, where Square Wave Voltammetry (SWV)-based immunosensing was coupled CuNCs growth [179] (Fig. 7B). The capturing Ab (Ab1) is immobilized on a glassy carbon electrode modified with Au nanoparticles (AuNPs), to bind PSA; the secondary Ab (Ab2) binds PSA on a different epitope of the Ab1. The novelty of the work is the use of BSA-templated CuNCs carried on platinum NPs and modified with Ab2. Thus, after the immunocomplex formation (Ab1-PSA-Ab2), catalytic signal amplification occurs, mediated by presence of Pt and Cu nanostructures. The recorded current is due to Cu^{2+} reduction at the electrode. The proposed immunosensor works in a wide linear range from 0.5 pg mL^{-1} to 100 ng mL^{-1} displaying a LOD of 145.69 fg mL^{-1} (S/N = 3). In addition, the assay demonstrated good response in clinical serum samples; compared to reference ELISA assays the two methods displayed from %RSD of 5.0% and 5.5%, respectively, thus good accuracy and an acceptable reliability for PSA analysis in real practice.

The detection of stimulated lipoprotein receptor (LSR), a biomarker closely related to ovarian cancer, deals with a photoelectrochemical (PEC)–colorimetric immunoassay [180]. Basically, the PEC response is reduced when the Antigen-Antibody reaction takes place. At the same time, color variations in Leuco-MB functionalized colorimetric poly (vinyl alcohol) (PVA) film occurs, providing a dual mechanism and independent signal transduction. The immunoassay is in a simple direct format, *i.e.*, the Ab, immobilized on the transducer surface, directly binds the Ag, added in solution. In detail, the immunoreaction takes place on the CuNCs, grown on several layers of TiO_2 (mixed TiO_2 mesocrystals junction (MMMJ)). CuNCs improve photoelectrochemical colorimetric properties and the catalytic activity of hydrogen peroxide (H_2O_2) that catalyzes Leuco-MB conversion from colorless to blue. When the antibody and the target antigen are captured onto the MMMJ, PEC properties and catalytic activities are inhibited. Spiked human serum samples with LSR, at sub ng/ml concentration level, provided excellent recovery (in the range from 98.4% to 100.7%). The assay analytical parameters are listed in Table 3.

Behind biosensing-based approaches, disposable platforms can be combined with CuNCs use, to improve test analytical performances, in ELISA-like assays. The sandwich immunoassay format is quite common for protein detection. In particular, Immunoglobulins (Ig) and cancer biomarkers like prostate-specific antigen (PSA), matrix metalloproteinase-7 (MMP7) detection has been addressed, by fluorescent, photoelectrochemical (PEC) and electrochemical *i.e.*, potentiometric analysis respectively. A fluorescent ELISA platform for IgG analysis with a new strategy for *in-situ i.e.*, in solution synthesis of CuNCs, is reported. A sandwich assay format is used, where Alkaline Phosphatase (ALP) is bound to the secondary Ab and catalyzes the hydrolysis of ascorbic acid 2-phosphate (AAP) leading to ascorbic acid, that, in presence of Cu^{2+} and the DNA template, allows the *in situ* growth of CuNCs [181] with fluorescence emission. A LOD of 7 pg mL^{-1} is achieved in IgG standard solutions. This novel, easy-to-use and cost-effective fluorescent ELISA platform, led to improved performances with respect to the common commercial ELISA kit and can be transferred to other analytes, if validity in real matrices is further explored.

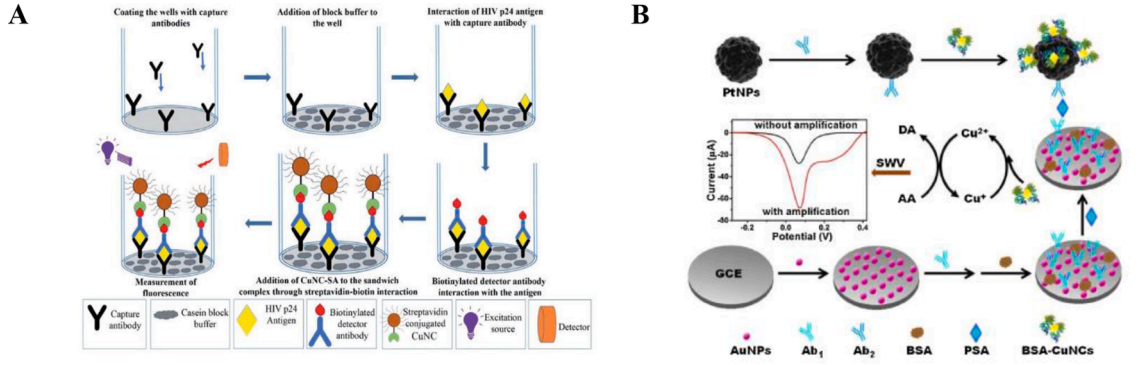

Fig. 7. Schematic illustration of CuNCs immunoassay-based detection strategies (A) according to the assay strategy proposed by Kurdekar's et al. reprinted from Ref. [178]., with permission of Royal Society of Chemistry; (B) according to the assay strategy proposed by Lihua Zhao and Zhanfang Ma, reprinted from Ref. [179], with permission of Elsevier B.V.

PSA is detected by a PEC-CuNCs-based immunoassay employing a Carbon Dots/g-C_3N_4 [182], while MMP7, involved in cancer progression, was quantitatively detected by potentiometric immunoassay using copper ion-selective electrode (Cu-ISE) with a portable detector [183]. Cu^{2+}, under acidic conditions, was released from CuCNs formed at the immunocomplex, where the secondary Ab was linked to a short nucleic acid sequence, acting as probe for further hybridization reaction cycles forming dsDNA structures, promoting CuCNs growth. A dynamic linear range of 0.01–100 ng mL^{-1} with a detection limit of 5.3 pg mL^{-1} MMP7 was achieved in human serum samples.

Behind the cancer biomarker MMP7, the quantitative analysis of cardiac troponin T (cTnT), an important marker of Acute Myocardial Infarction (AMI) is reported by a PEC approach [183]. Here CuCNs were synthesized on BSA, eventually encapsulated in liposomes for further labeling of antibodies to their external surface. After the sandwich immunocomplexing, the confined liposomal labels were lysed to release the CuNCs and numerous Cu^{2+} ions, free to interact with the ITO electrode modified with quantum dots (QD) modifying the photocurrent [183]. The photocurrent signal decreased linearly with the increasing cTnT concentrations from 0.1 to 2 pg mL^{-1}, with a LOD of 0.03 pg mL^{-1} in standard solutions. The details relative to the CuNCs immunoassay-based detection strategies are reported in Table 3. Finally, considering the CuCNs growth on some proteins, carrying suitable characteristics, one may think of simple and direct antibody-free assays. We very recently reported on sensitive and selective Human Serum Albumin (HSA) fluorimetric detection in body fluids, *i.e.*, urine with interest in kidney related diseases. HSA in different matrices was detected, obtaining excellent limits of detection: 2.48 ± 0.07 mg L^{-1} (in H_2O), 1.8 ± 0.1 mg L^{-1} (in human serum) and 0.62 ± 0.03 mg L^{-1} (in urine). This confirms the potentialities of these very powerful nanostructures [97].

3.4. Ratiometric fluorescent sensing based on CuNCs

Recently, ratiometric fluorescent methods have attracted growing research interest [185]. Generally, this emerging fluorescent technique exploits double tunable emission characteristics of two fluorescence species [186].

In order to design a ratiometric sensor, a suitable reference probe should be choice [187]. Emerging nanomaterial used for the development of ratiometric fluorescent probe are CuNCs [188]. Generally, the CuNCs-based ratiometric methods take advantage of the combination of CuNCs PL properties with additionally fluorescent species (*e.g.*. dye, QDs, NMs etc.) [189]. The fabrication of ratiometric fluorescent probes usually exploits several photophysical properties including internal charge transfer (ICT), fluorescence resonance energy transfer (FRET), monomer–excimer formation, and excited-state intramolecular proton transfer (ESIPT) [190]. Despite the gain in terms of method accuracy, the reports of ratiometric fluorescent sensor based on CuNCs, are limited. This is probably due to the lack of effective means to tune emission wavelength of the synthesized Cu NCs [191] . However, we report an interesting study on ratiometric fluorescence sensing platform developed by Wang and its collaborators [192]. This work was based on the sensing platform developed in which GSH-CuNCs and o-phenylenediamine was integrated into same device. This label-free fluorescent ratiometric assay allowed very sensitively and simultaneously detection of Cu^{2+} and kojic acid. This method paved the way for future application in real sample analysis closely concerned with human health [192].

4. Biological application of CuNCs

The biocompatibility and the low toxicity of CuNCs enable their application as fluorophores for *in vitro* and *in vivo* biological imaging by using different kinds of templates for the preparation of CuNCs. Numerous works reported blue emitting CuNCs for the labeling of various kinds of cell lines, including human and cancerous cells, as well as microorganism cells [193–195]. In order to verify the compatibility of CuNCs in biological systems, diverse tests were performed in biological samples like blood or serum [99,196]. An interesting study was conducted by Mukherjee's group in which Glutathione (GSH)-CuNCs were employed to perform cell viability and uptake assays on three cancerous cell lines, HeLa (malignant immortal cell line derived from cervical cancer), A549 (human lung carcinoma) and MDAMB-231 (human breast adenocarcinoma) [197]. They demonstrated the low toxicity of CuNCs localizing the nanoclusters close to the nucleus by laser scanning confocal microscopy. The same procedure was followed on *Bacillus subtilis* cells by Kailasa's group for *in vitro* imaging tests [32]. In the last years, great advances in the application of CuNCs combined with *in vivo* imaging strategies, have been reached (Table 4). One of the most innovative research is represented by the synthesis of radioactive BSA-CuNCs conjugated with the Luteinizing Hormone Releasing Hormone (LHRH) whose receptor is overexpressed in some cancer cells such as breast, ovarian, prostate, lung, and hepatic ones. The 64CuNCs@BSA-LHRH structure was thought to be used as a contrast agent for *in vivo* PET imaging and the uptake by tumor cells in a primary lung cancer model [90]. Theranostic applications based on the use of CuNCs are instead more common [6,43]. For example, a hydrogel-based anticancer carrier containing CuNCs and Cisplatin were exploited for mammalian cell uptake monitoring [198]. Moreover, CuNCs was used as a biological dye to stain proteins or oligonucleotides in gel electrophoresis [199] and cells in flow cytometry [200]. Copper, like other noble metals, is known also for its antibacterial properties; therefore, CuNCs were used for their antimicrobial action [201].

5. Conclusions and future perspectives

In this review, we focused on the remarkable progress in the synthesis and use of fluorescent copper nanoclusters combined with different detection strategies. We first evaluated diverse aspects that influence the photoluminescent properties of CuNCs, in particular size, surface ligands, and reaction environment. The synthesis of CuNCs can be effectively controlled by using a template-assisted approach. Nucleic acids, proteins, polymers, peptides, and small molecules are usually employed to reduce copper ions, stabilize and protect the growth of nanoclusters. In particular, nucleic acids, beside being excellent templates, are powerful biological recognition elements for bioanalytical assay development. Here, we discussed the combination of oligonucleotide sequences, as capture probes, and copper nanoclusters in CuNCs DNA-based detection strategies. We at first reported the CuNCs-based assays classified according to the capture probe used (*i.e.*, DNA, aptamer, antibody) and, consequently, we discussed the CuNCs-based assays diversified depending on the transduction element (*i.e.,* electrochemical, photoelectrochemical, colorimetric). Then we analyzed the biological application of copper nanoclusters. Despite the numerous advantages in terms of excellent fluorescent properties, cost effectiveness, selectivity, sensitivity, rapidity in the response, versatility and environmental-benign, the use of CuNCs for analytical applications is mostly unexplored, with a low number of publications about immunobased or electrochemical-based assays involving CuNCs in the detection strategy. Consequently, this research area offers considerable margins of improvement and new investigations. Firstly, large scale synthesis does not allow to obtain CuNCs with uniform size distribution. This mainly occurs in DNA-CuNCs synthesis where it is necessary to pay more attention to the experimental condition to guarantee a long-term stability of DNA-templated CuNCs. Secondly, the CuNCs formation mechanism on nucleotides template is still unknown. In addition, CuNCs signal can be quenched by many biomolecules and this could influence the system selectivity. Finally, more studies are expected for practical applications. For example, the development of CuNCs-based disposable devices, *i.e.*, paper-based assay systems, as well as the combination of CuNCs with antibody-free biomimetic receptors, such as molecularly imprinted polymers (MIP), could lead to a great advantage in the fast and cost-effective target analyte detection.

Table 4
Biological application of CuNCs.

Application	Template	Target	$\lambda_{ex}/\lambda_{em}$	Sample	Linear range	LOD	Q.Y.	Refs.
In vitro Bioimaging	Lysozyme	–	375/450 nm	HeLa cells, Human blood	–	–	14%	[99]
In vitro Bioimaging	Tannic acid	Fe^{3+}	360/480 nm	Serum and living cell (A549)	10 nM-10 μM	10nM	18%	[196]
In vitro Bioimaging	GSH	Fe^{3+}	340/430 nm	HeLa, A549, MDAMB-231 human cells	10 nM-50 μM	25 nM	6%	[197]
In vitro Bioimaging	Egg white	Thiram and paraquat	340/600 nm	Food samples and *Bacillus subtilis*	0.5- 1000 μM (thiram), 0.2–1000 μM (paraquat)	70 nM (thiram) 49 nM (paraquat)	6.7%	[32]
In vivo Bioimaging	BSA	Orthopedic lung tumor	488/640 nm	Mice, MRC-5 and A549 cells	–	–	–	[90]
Theranostic	PVP	Cisplatin	365/650 nm	HeLa cells	1.5–8.4 mg L^{-1}	–	7.2%	[198]
Biological dye	DNA	DNA	343/584 nm	–	–	–	–	[199]
Flow cytometry	L-cysteine (NCs1) and GSH (NCs2)	Tetracycline	368/493 nm (NCs1) 373/595 nm (NCs2)	HeLa cells	–	5.6 μM (NCs1), 8.4 μM (NCs2)	5.8%–3.6%	[200]
Antimicrobial action	GSH	–	588/488 nm	*E. coli*, DH5α	–	–	1.3×10^{-4}	[201]

Declaration of Competing Interest

The authors declare that they have no known competing financial interests or personal relationships that could have appeared to influence the work reported in this paper.

References

[1] G.E. Giacomazzo, P. Palladino, C. Gellini, G. Salerno, V. Baldoneschi, A. Feis, S. Scarano, M. Minunni, B. Richichi, A straightforward synthesis of phenyl boronic acid (PBA) containing BODIPY dyes: new functional and modular fluorescent tools for the tethering of the glycan domain of antibodies, RSC Adv. 9 (2019) 30773–30777, https://doi.org/10.1039/c9ra07608e.

[2] G. Salerno, S. Scarano, M. Mamusa, M. Consumi, S. Giuntini, A. Macagnano, S. Nativi, M. Fragai, M. Minunni, D. Berti, A. Magnani, C. Nativi, B. Richichi, A small heterobifunctional ligand provides stable and water dispersible core-shell CdSe/ZnS quantum dots (QDs), Nanoscale 10 (2018) 19720–19732, https://doi.org/10.1039/c8nr05566a.

[3] S. Hong, Y.A. Kuo, T.D. Nguyen, Y.I. Chen, Y.L. Liu, P.B. Shankar, H.C. Yeh, D. Fixler, S. Wachsmann-Hogiu, E.M. Goldys, Array-based differential sensing of cancer cells using DNA-templated silver nanoclusters. Nanoscale Imaging, Sensing, and Actuation for Biomedical Applications XVII, SPIE, 2020, p. 34, https://doi.org/10.1117/12.2540132.

[4] D. Sahu, P. Mohapatra, S.K. Swain, Highly orange fluorescence emission by water soluble gold nanoclusters for "turn off" sensing of Hg^{2+} ion, J. Photochem. Photobiol. A Chem. 386 (2020), 112098, https://doi.org/10.1016/j.jphotochem.2019.112098.

[5] P. Vaid, P. Raizada, A.K. Saini, R.V. Saini, Biogenic silver, gold and copper nanoparticles - a sustainable green chemistry approach for cancer therapy, Sustain. Chem. Pharm. 16 (2020), 100247, https://doi.org/10.1016/j.scp.2020.100247.

[6] W.F. Lai, W.T. Wong, A.L. Rogach, Development of copper nanoclusters for *in vitro* and *in vivo* theranostic applications, Adv. Mater. 32 (2020) 1–21, https://doi.org/10.1002/adma.201906872.

[7] Q. Zhang, M. Yang, Y. Zhu, C. Mao, Metallic nanoclusters for cancer imaging and therapy, Curr. Med. Chem. 24 (2017), https://doi.org/10.2174/0929867324666170331122757, 1–1.

[8] M. Zhou, M. Tian, C. Li, Copper-based nanomaterials for cancer imaging and therapy, Bioconjug. Chem. 27 (2016) 1188–1199, https://doi.org/10.1021/acs.bioconjchem.6b00156.

[9] J. Benavides, I. Quijada-Garrido, O. García, The synthesis of switch-off fluorescent water-stable copper nanocluster Hg^{2+} sensors: via a simple one-pot approach by an *in situ* metal reduction strategy in the presence of a thiolated polymer ligand template, Nanoscale 12 (2020) 944–955, https://doi.org/10.1039/c9nr08439h.

[10] K.T. Prakash, N. Singh, V. Venkatesh, Synthesis of novel luminescent copper nanoclusters with substituent driven self-assembly and aggregation induced emission (AIE), Chem. Commun. 55 (2019) 322–325, https://doi.org/10.1039/c8cc09109a.

[11] Z.S. Kardar, F. Shemirani, R. Zadmard, Determination of iron(II) and iron(III) via static quenching of the fluorescence of tryptophan-protected copper nanoclusters, Microchim. Acta 187 (2020) 1–9, https://doi.org/10.1007/s00604-019-4067-4.

[12] Y. Lu, W. Chen, Sub-nanometre sized metal clusters: from synthetic challenges to the unique property discoveries, Chem. Soc. Rev. 41 (2012) 3594–3623, https://doi.org/10.1039/c2cs15325d.

[13] M. Zhao, L. Sun, R.M. Crooks, Preparation of Cu nanoclusters within dendrimer templates, J. Am. Chem. Soc. 120 (1998) 4877–4878, https://doi.org/10.1021/ja980438n.

[14] L. Balogh, D.A. Tomalia, Nanocomposites . 1. Synthesis of zerovalent copper nanoclusters, J. Am. Chem. Soc. 120 (1998) 7355–7356.

[15] X. Hu, T. Liu, Y. Zhuang, W. Wang, Y. Li, W. Fan, Y. Huang, Recent advances in the analytical applications of copper nanoclusters, TrAC Trends Anal. Chem. 77 (2016) 66–75, https://doi.org/10.1016/j.trac.2015.12.013.

[16] A. Rotaru, S. Dutta, E. Jentzsch, K. Gothelf, A. Mokhir, Selective dsDNA-templated formation of copper nanoparticles in solution, Angew. Chem. Int. Ed. 49 (2010) 5665–5667, https://doi.org/10.1002/anie.200907256.

[17] A. Nain, Y.T. Tseng, S.C. Wei, A.P. Periasamy, C.C. Huang, F.G. Tseng, H. T. Chang, Capping 1,3-propanedithiol to boost the antibacterial activity of protein-templated copper nanoclusters, J. Hazard. Mater. 389 (2020), 121821, https://doi.org/10.1016/j.jhazmat.2019.121821.

[18] H. Huang, H. Li, A.J. Wang, S.X. Zhong, K.M. Fang, J.J. Feng, Green synthesis of peptide-templated fluorescent copper nanoclusters for temperature sensing and cellular imaging, Analyst 139 (2014) 6536–6541, https://doi.org/10.1039/c4an01757a.

[19] X. Yang, Y. Feng, S. Zhu, Y. Luo, Y. Zhuo, Y. Dou, One-step synthesis and applications of fluorescent Cu nanoclusters stabilized by L-cysteine in aqueous solution, Anal. Chim. Acta 847 (2014) 49–54, https://doi.org/10.1016/j.aca.2014.07.019.

[20] S. Kolay, D. Bain, S. Maity, A. Devi, A. Patra, R. Antoine, Self-assembled metal nanoclusters: driving forces and structural correlation with optical properties, (2022).

[21] N. Goswami, A. Giri, M.S. Bootharaju, P.L. Xavier, T. Pradeep, S.K. Pal, Copper quantum clusters in protein matrix: potential sensor of Pb^{2+} ion, Anal. Chem. 83 (2011) 9676–9680, https://doi.org/10.1021/ac202610e.

[22] K. Yang, Y. Wang, C. Lu, X. Yang, Ovalbumin-directed synthesis of fluorescent copper nanoclusters for sensing both vitamin B1 and doxycycline, J. Lumin. 196 (2018) 181–186, https://doi.org/10.1016/j.jlumin.2017.12.038.

[23] Z. Cai, H. Li, J. Wu, L. Zhu, X. Ma, C. Zhang, Ascorbic acid stabilised copper nanoclusters as fluorescent sensors for detection of quercetin, RSC Adv. 10 (2020) 8989–8993, https://doi.org/10.1039/d0ra01265c.

[24] S. Chen, Y. Wang, L. Feng, Specific detection and discrimination of dithiocarbamates using CTAB-encapsulated fluorescent copper nanoclusters, Talanta 210 (2020), 120627, https://doi.org/10.1016/j.talanta.2019.120627.

[25] A. Yousefzadeh, J. Hassanzadeh, S.M.J. Mousavi, M. Yousefzadeh, Surface molecular imprinting and powerfully enhanced chemiluminescence emission by Cu nanoclusters/MOF composite for detection of tramadol, Sens. Actuators B Chem. 286 (2019) 154–162, https://doi.org/10.1016/j.snb.2019.01.155.

[26] R.S. Aparna, J.S. Anjali Devi, R.R. Anjana, J. Nebu, S. George, Zn(II) ion modulated red emitting copper nanocluster probe for the fluorescence turn on sensing of RDX, Sens. Actuators B Chem. 291 (2019) 298–305, https://doi.org/10.1016/j.snb.2019.04.051.

[27] C. Wang, Y. Yao, Q. Song, Interfacial synthesis of polyethyleneimine-protected copper nanoclusters: size-dependent tunable photoluminescence, pH sensor and bioimaging, Colloids Surf. B Biointerfaces 140 (2016) 373–381, https://doi.org/10.1016/j.colsurfb.2016.01.001.

[28] Z. Cai, C. Zhang, K. Jia, L-tyrosine protected Cu nanoclusters for reversible pH-sensors, Chem. Pap. 74 (2020) 1831–1838, https://doi.org/10.1007/s11696-019-01027-x.

[29] G. Zhang, T. Xu, H. Du, Y. Qiao, X. Guo, L. Shi, Y. Zhang, S. Shuang, C. Dong, H. Ma, A reversible fluorescent pH-sensing system based on the one-pot synthesis of natural silk fibroin-capped copper nanoclusters, J. Mater. Chem. C 4 (2016) 3540–3545, https://doi.org/10.1039/c6tc00314a.

[30] Y. Cheng, S. Deng, F. Sun, Y.H. Zhou, Synthesis of luminescent Cu 9 S 5 nanoclusters from copper-2,5-dimercapto-1,3,4-thiadiazole coordination polymer as pH sensor, J. Lumin. 210 (2019) 38–46, https://doi.org/10.1016/j.jlumin.2019.02.014.

[31] J. Ye, X. Dong, H. Jiang, X. Wang, An intracellular temperature nanoprobe based on biosynthesized fluorescent copper nanoclusters, J. Mater. Chem. B 5 (2017) 691–696, https://doi.org/10.1039/c6tb02751b.

[32] J.R. Bhamore, S. Jha, A.K. Mungara, R.K. Singhal, D. Sonkeshariya, S.K. Kailasa, One-step green synthetic approach for the preparation of multicolor emitting copper nanoclusters and their applications in chemical species sensing and bioimaging, Biosens. Bioelectron. 80 (2016) 243–248, https://doi.org/10.1016/j.bios.2016.01.066.

[33] X. Gao, X. Zhuang, C. Tian, H. Liu, W.F. Lai, Z. Wang, X. Yang, L. Chen, A. L. Rogach, A copper nanocluster incorporated nanogel: confinement-assisted emission enhancement for zinc ion detection in living cells, Sens. Actuators B Chem. 307 (2020), 127626, https://doi.org/10.1016/j.snb.2019.127626.

[34] T. Qing, K. Zhang, Z. Qing, X. Wang, C. Long, P. Zhang, H. Hu, B. Feng, Recent progress in copper nanocluster-based fluorescent probing: a review, Microchim. Acta (2019) 186, https://doi.org/10.1007/s00604-019-3747-4.

[35] S. Pramanik, L. Khamari, S. Nandi, S. Mukherjee, Discriminating single base pair mismatches in DNA using glutathione-templated copper nanoclusters, J. Phys. Chem. C 123 (2019) 29047–29056, https://doi.org/10.1021/acs.jpcc.9b10069.

[36] X.S. Peng, S.Y. Chen, L.J. Ou, F.W. Luo, S.W. Qin, A.M. Sun, Hairpin loop-enhanced fluorescent copper nanoclusters and application in S1 nuclease detection, Analyst 143 (2018) 415–419, https://doi.org/10.1039/c7an01725a.

[37] A. Mao, C. Wei, Cytosine-rich ssDNA-templated fluorescent silver and copper/silver nanoclusters: optical properties and sensitive detection for mercury(II), Microchim. Acta (2019) 186, https://doi.org/10.1007/s00604-019-3658-4.

[38] Y. An, Y. Ren, M. Bick, A. Dudek, E. Hong-Wang Waworuntu, J. Tang, J. Chen, B. Chang, Highly fluorescent copper nanoclusters for sensing and bioimaging, Biosens. Bioelectron. (2020) 154, https://doi.org/10.1016/j.bios.2020.112078.

[39] S. Shahsavari, S. Hadian-Ghazvini, F. Hooriabad Saboor, I. Menbari Oskouie, M. Hasany, A. Simchi, A.L. Rogach, Ligand functionalized copper nanoclusters for versatile applications in catalysis, sensing, bioimaging, and optoelectronics, Mater. Chem. Front. 3 (2019) 2326–2356, https://doi.org/10.1039/c9qm00492k.

[40] L. Farzin, M. Shamsipur, L. Samandari, S. Sadjadi, S. Sheibani, Biosensing strategies based on organic-scaffolded metal nanoclusters for ultrasensitive detection of tumor markers, Talanta 214 (2020), 120886, https://doi.org/10.1016/j.talanta.2020.120886.

[41] Q. Cao, J. Li, E. Wang, Recent advances in the synthesis and application of copper nanomaterials based on various DNA scaffolds, Biosens. Bioelectron. 132 (2019) 333–342, https://doi.org/10.1016/j.bios.2019.01.046.

[42] R. Gui, H. Jin, X. Bu, Y. Fu, Z. Wang, Q. Liu, Recent advances in dual-emission ratiometric fluorescence probes for chemo/biosensing and bioimaging of biomarkers, Coord. Chem. Rev. 383 (2019) 82–103, https://doi.org/10.1016/j.ccr.2019.01.004.

[43] K.B. Busi, M. Palanivel, K.K. Ghosh, W.B. Ball, B. Gulyás, P. Padmanabhan, S. Chakrabortty, The multifarious applications of copper nanoclusters in biosensing and bioimaging and their translational role in early disease detection, Nanomaterials (2022) 12, https://doi.org/10.3390/nano12030301.

[44] D.M. Wood, N.W. Ashcroft, Quantum size effects in the optical properties of small metallic particles, Phys. Rev. B 25 (1982) 6255–6274, https://doi.org/10.1103/PhysRevB.25.6255.

[45] Z. Wang, B. Chen, A.L. Rogach, Synthesis, optical properties and applications of light-emitting copper nanoclusters, Nanoscale Horiz. 2 (2017) 135–146, https://doi.org/10.1039/c7nh00013h.

[46] M.V. Pavliuk, S. Gutiérrez Álvarez, Y. Hattori, M.E. Messing, J. Czapla-Masztafiak, J. Szlachetko, J.L. Silva, C.M. Araujo, D.L. Fernandes, L. Lu, C. J. Kiely, M. Abdellah, P. Nordlander, J. Sá, Hydrated electron generation by excitation of copper localized surface plasmon resonance, J. Phys. Chem. Lett. 10 (2019) 1743–1749, https://doi.org/10.1021/acs.jpclett.9b00792.

[47] L.V.Q. Garrido, J.M. Gonçalves, J.C. Rocha, E.L. Bastos, H.E. Toma, V. M. Zamarion, Intriguing plasmonic and fluorescence duality in copper nanoparticles, Plasmonics (2020), https://doi.org/10.1007/s11468-020-01143-5.

[48] A. Ziashahabi, T. Ghodselahi, M.H. Saani, Localized surface plasmon resonance properties of copper nano-clusters: a theoretical study of size dependence, J. Phys. Chem. Solids 74 (2013) 929–933, https://doi.org/10.1016/j.jpcs.2013.02.009.

[49] Y.Z. Lu, W.T. Wei, W. Chen, Copper nanoclusters: synthesis, characterization and properties, Chinese Sci. Bull. 57 (2012) 41–47, https://doi.org/10.1007/s11434-011-4896-y.

[50] D. Li, Z. Chen, X. Mei, Fluorescence enhancement for noble metal nanoclusters, Adv. Colloid Interface Sci. 250 (2017) 25–39, https://doi.org/10.1016/j.cis.2017.11.001.

[51] C. Vázquez-Vázquez, M. Bañobre-López, A. Mitra, M.A. López-Quintela, J. Rivas, Synthesis of small atomic copper clusters in microemulsions, Langmuir 25 (2009) 8208–8216, https://doi.org/10.1021/la900100w.

[52] Z. Luo, X. Yuan, Y. Yu, Q. Zhang, D.T. Leong, J.Y. Lee, J. Xie, From aggregation-induced emission of Au(I)-thiolate complexes to ultrabright Au(0)@Au(I)-thiolate core-shell nanoclusters, J. Am. Chem. Soc. 134 (2012) 16662–16670, https://doi.org/10.1021/ja306199p.

[53] Z. Wu, R. Jin, On the ligand's role in the fluorescence of gold nanoclusters, Nano Lett. 10 (2010) 2568–2573, https://doi.org/10.1021/nl101225f.

[54] Z. Wang, A.S. Susha, B. Chen, C. Reckmeier, O. Tomanec, R. Zboril, H. Zhong, A. L. Rogach, Poly(vinylpyrrolidone) supported copper nanoclusters: glutathione enhanced blue photoluminescence for application in phosphor converted light emitting devices, Nanoscale 8 (2016) 7197–7202, https://doi.org/10.1039/c6nr00806b.

[55] M. Cui, G. Song, C. Wang, Q. Song, Synthesis of cysteine-functionalized water-soluble luminescent copper nanoclusters and their application to the determination of chromium(VI), Microchim. Acta 182 (2015) 1371–1377, https://doi.org/10.1007/s00604-015-1458-z.

[56] C. Wang, Y. Huang, Green route to prepare biocompatible and near infrared thiolate-protected copper nanoclusters for cellular imaging, Nano 8 (2013), https://doi.org/10.1142/S1793292013500549.

[57] R. Rajamanikandan, M. Ilanchelian, Red emitting human serum albumin templated copper nanoclusters as effective candidates for highly specific biosensing of bilirubin, Mater. Sci. Eng. C 98 (2019) 1064–1072, https://doi.org/10.1016/j.msec.2019.01.048.

[58] Z. Miao, W. Hou, M. Liu, Y. Zhang, S. Yao, BSA capped bi-functional fluorescent Cu nanoclusters as pH sensor and selective detection of dopamine, New J. Chem. 42 (2018) 1446–1456, https://doi.org/10.1039/c7nj03524a.

[59] J. Feng, Y. Chen, Y. Han, J. Liu, S. Ma, H. Zhang, X. Chen, PH-Regulated synthesis of trypsin-templated copper nanoclusters with blue and yellow fluorescent emission, ACS Omega 2 (2017) 9109–9117, https://doi.org/10.1021/acsomega.7b01052.

[60] W. Wang, F. Leng, L. Zhan, Y. Chang, X.X. Yang, J. Lan, C.Z. Huang, One-step prepared fluorescent copper nanoclusters for reversible pH-sensing, Analyst 139 (2014) 2990–2993, https://doi.org/10.1039/c4an00113c.

[61] C. Wang, C. Wang, L. Xu, H. Cheng, Q. Lin, C. Zhang, Protein-directed synthesis of pH-responsive red fluorescent copper nanoclusters and their applications in cellular imaging and catalysis, Nanoscale 6 (2014) 1775–1781, https://doi.org/10.1039/c3nr04835g.

[62] J. Yuan, L. Wang, Y. Wang, J. Hao, Stimuli-responsive fluorescent nanoswitches: solvent-induced emission enhancement of copper nanoclusters, Chem. A Eur. J. 26 (2020) 3545–3554, https://doi.org/10.1002/chem.201905094.

[63] Y. Ling, J.J. Wu, Z.F. Gao, N.B. Li, H.Q. Luo, Enhanced emission of polyethyleneimine-coated copper nanoclusters and their solvent effect, J. Phys. Chem. C 119 (2015) 27173–27177, https://doi.org/10.1021/acs.jpcc.5b09488.

[64] N. Vilar-Vidal, M.C. Blanco, M.A. López-Quintela, J. Rivas, C. Serra, Electrochemical synthesis of very stable photoluminescent copper clusters, J. Phys. Chem. C (2010) 15924–15930, https://doi.org/10.1021/jp911380s. American Chemical Society.

[65] A. Han, L. Xiong, S. Hao, Y. Yang, X. Li, G. Fang, J. Liu, Y. Pei, S. Wang, Highly bright self-assembled copper nanoclusters: a novel photoluminescent probe for sensitive detection of histamine, Anal. Chem. 90 (2018) 9060–9067, https://doi.org/10.1021/acs.analchem.8b01384.

[66] H.H. Deng, K.L. Li, Q.Q. Zhuang, H.P. Peng, Q.Q. Zhuang, A.L. Liu, X.H. Xia, W. Chen, An ammonia-based etchant for attaining copper nanoclusters with green fluorescence emission, Nanoscale 10 (2018) 6467–6473, https://doi.org/10.1039/c7nr09449c.

[67] N.K. Das, S. Mukherjee, Size-controlled atomically precise copper nanoclusters: synthetic protocols, spectroscopic properties and applications, Phys. Sci. Rev. 3 (2018) 1–22, https://doi.org/10.1515/psr-2017-0081.

[68] S. Huseyinova, J. Blanco, F.G. Requejo, J.M. Ramallo-López, M.C. Blanco, D. Buceta, M.A. López-Quintela, Synthesis of highly stable surfactant-free Cu5 clusters in water, J. Phys. Chem. C 120 (2016) 15902–15908, https://doi.org/10.1021/acs.jpcc.5b12227.

[69] C. Wang, H. Cheng, Y. Sun, Q. Lin, C. Zhang, Rapid sonochemical synthesis of luminescent and paramagnetic copper nanoclusters for bimodal bioimaging, ChemNanoMat 1 (2015) 27–31, https://doi.org/10.1002/cnma.201500004.

[70] R. Gui, J. Sun, X. Cao, Y. Wang, H. Jin, Multidentate polymers stabilized water-dispersed copper nanoclusters: facile photoreduction synthesis and selective fluorescence turn-on response, RSC Adv. 4 (2014) 29083–29088, https://doi.org/10.1039/c4ra03606a.

[71] R. Rajamanikandan, M. Ilanchelian, Protein-protected red emittive copper nanoclusters as a fluorometric probe for highly sensitive biosensing of creatinine, Anal. Methods 10 (2018) 3666–3674, https://doi.org/10.1039/c8ay00827b.

[72] D. Zhang, Y. Fang, Z. Miao, M. Ma, X. Du, S. Takahashi, J.I. Anzai, Q. Chen, Direct electrodeposion of reduced graphene oxide and dendritic copper nanoclusters on glassy carbon electrode for electrochemical detection of nitrite, Electrochim. Acta 107 (2013) 656–663, https://doi.org/10.1016/j.electacta.2013.06.015.

[73] C. Wang, H. Cheng, Y. Huang, Z. Xu, H. Lin, C. Zhang, Facile sonochemical synthesis of pH-responsive copper nanoclusters for selective and sensitive detection of Pb^{2+} in living cells, Analyst 140 (2015) 5634–5639, https://doi.org/10.1039/c5an00741k.

[74] C.A. Chen, C.C. Wang, Y.J. Jong, S.M. Wu, Label-free fluorescent copper nanoclusters for genotyping of deletion and duplication of duchenne muscular dystrophy, Anal. Chem. 87 (2015) 6228–6232, https://doi.org/10.1021/acs.analchem.5b00918.

[75] N. Russo, M. Toscano, A. Grand, Gas-phase theoretical prediction of the metal affinity of copper(I) ion for DNA and RNA bases, J. Mass Spectrom. 38 (2003) 265–270, https://doi.org/10.1002/jms.436.

[76] X. Wang, P. Hu, Z. Wang, Q. Liu, T. Xu, M. Kou, K. Huang, P. Chen, A fluorescence strategy for silver ion assay via cation exchange reaction and formation of poly

(thymine)-templated copper nanoclusters, Anal. Sci. 35 (2019) 917–922, https://doi.org/10.2116/analsci.19P036.
[77] X. Bu, Y. Fu, X. Jiang, H. Jin, R. Gui, Self-assembly of DNA-templated copper nanoclusters and carbon dots for ratiometric fluorometric and visual determination of arginine and acetaminophen with a logic-gate operation, Microchim. Acta (2020) 187, https://doi.org/10.1007/s00604-020-4146-6.
[78] B. Han, R. Xiang, X. Hou, M. Yu, T. Peng, Y. Li, G. He, One-step rapid synthesis of single thymine-templated fluorescent copper nanoclusters for "turn on" detection of Mn^{2+}, Anal. Methods 9 (2017) 2590–2595, https://doi.org/10.1039/c7ay00625j.
[79] H. Zhao, J. Dong, F. Zhou, B. Li, One facile fluorescence strategy for sensitive detection of endonuclease activity using DNA-templated copper nanoclusters as signal indicators, Sens. Actuators B Chem. 238 (2017) 828–833, https://doi.org/10.1016/j.snb.2016.07.083.
[80] J. Pang, Y. Lu, X. Gao, L. He, J. Sun, F. Yang, Z. Hao, Y. Liu, DNA-templated copper nanoclusters as a fluorescent probe for fluoride by using aluminum ions as a bridge, Microchim. Acta 186 (2019) 1–9, https://doi.org/10.1007/s00604-019-3468-8.
[81] X.G. Li, F. Zhang, Y. Gao, Q.M. Zhou, Y. Zhao, Y. Li, J.Z. Huo, X.J. Zhao, Facile synthesis of red emitting 3-aminophenylboronic acid functionalized copper nanoclusters for rapid, selective and highly sensitive detection of glycoproteins, Biosens. Bioelectron. 86 (2016) 270–276, https://doi.org/10.1016/j.bios.2016.06.054.
[82] C. Muñoz-Bustos, A. Tirado-Guízar, F. Paraguay-Delgado, G. Pina-Luis, Copper nanoclusters-coated BSA as a novel fluorescence sensor for sensitive and selective detection of mangiferin, Sens. Actuators B Chem. 244 (2017) 922–927, https://doi.org/10.1016/j.snb.2017.01.071.
[83] G. Liu, W. He, C. Liu, Sensitive detection of uracil-DNA glycosylase (UDG) activity based on terminal deoxynucleotidyl transferase-assisted formation of fluorescent copper nanoclusters (CuNCs), Talanta 195 (2019) 320–326, https://doi.org/10.1016/j.talanta.2018.11.083.
[84] J. Cao, W. Wang, B. Bo, X. Mao, K. Wang, X. Zhu, A dual-signal strategy for the solid detection of both small molecules and proteins based on magnetic separation and highly fluorescent copper nanoclusters, Biosens. Bioelectron. 90 (2017) 534–541, https://doi.org/10.1016/j.bios.2016.10.021.
[85] S. Lisi, E. Fiore, S. Scarano, E. Pascale, Y. Boehman, F. Ducongé, S. Chierici, M. Minunni, E. Peyrin, C. Ravelet, Non-SELEX isolation of DNA aptamers for the homogeneous-phase fluorescence anisotropy sensing of tau proteins, Anal. Chim. Acta 1038 (2018) 173–181, https://doi.org/10.1016/j.aca.2018.07.029.
[86] S. Tombelli, M. Minunni, M. Mascini, Analytical applications of aptamers, Biosens. Bioelectron. 20 (2005) 2424–2434, https://doi.org/10.1016/J.BIOS.2004.11.006.
[87] C.A. Chen, C.C. Wang, Y.J. Jong, S.M. Wu, Label-free fluorescent copper nanoclusters for genotyping of deletion and duplication of Duchenne muscular dystrophy, Anal. Chem. 87 (2015) 6228–6232, https://doi.org/10.1021/acs.analchem.5b00918.
[88] T. Lalic, R.H.A.M. Vossen, J. Coffa, J.P. Schouten, M. Guc-Scekic, D. Radivojevic, M. Djurisic, M.H. Breuning, S.J. White, J.T. den Dunnen, Deletion and duplication screening in the DMD gene using MLPA, Eur. J. Hum. Genet. 13 (2005) 1231–1234, https://doi.org/10.1038/sj.ejhg.5201465.
[89] Y.L. Ankur Choksi, X. Zhang, G. Seong Heo, H. Luehmanna, Synthesis of temozolomide loaded copper nanoclusters for glioblastoma multiforme theranostics, (n.d.). http://jnm.snmjournals.org/content/59/supplement_1/1122.short (accessed August 5, 2020).
[90] F. Gao, P. Cai, W. Yang, J. Xue, L. Gao, R. Liu, Y. Wang, Y. Zhao, X. He, L. Zhao, G. Huang, F. Wu, Y. Zhao, Z. Chai, X. Gao, Ultrasmall [64Cu]Cu nanoclusters for targeting orthotopic lung tumors using accurate positron emission tomography imaging, ACS Nano 9 (2015) 4976–4986, https://doi.org/10.1021/nn507130k.
[91] Z. Yan, Q. Niu, M. Mou, Y. Wu, X. Liu, S. Liao, A novel colorimetric method based on copper nanoclusters with intrinsic peroxidase-like for detecting xanthine in serum samples, J. Nanoparticle Res. (2017) 19, https://doi.org/10.1007/s11051-017-3904-9.
[92] L. Xiaoqing, L. Ruiyia, L. Zaijun, Ultra sensitive and wide-range pH sensor based on the BSA-capped Cu nanoclusters fabricated by fast synthesis through the use of hydrogen peroxide additive, RSC Adv. 10 (2015) 2–8.
[93] C. Wang, C. Wang, L. Xu, H. Cheng, Q. Lin, C. Zhang, Protein-directed synthesis of pH-responsive red fluorescent copper nanoclusters and their applications in cellular imaging and catalysis, Nanoscale 6 (2014) 1775–1781, https://doi.org/10.1039/c3nr04835g.
[94] M. Chen, W. Li, H. Xiong, W. Wen, X. Zhang, S. Wang, Discrimination and ultrasensitive detection of β 2-agonists using copper nanoclusters as a fluorescent probe, Microchim. Acta 184 (2017) 3317–3324, https://doi.org/10.1007/s00604-017-2357-2.
[95] H.B. Wang, Y. Chen, N. Li, Y.M. Liu, A fluorescent glucose bioassay based on the hydrogen peroxide-induced decomposition of a quencher system composed of MnO2 nanosheets and copper nanoclusters, Microchim. Acta 184 (2017) 515–523, https://doi.org/10.1007/s00604-016-2045-7.
[96] S. Ghosh, N.K. Das, U. Anand, S. Mukherjee, Photostable copper nanoclusters: compatible Förster resonance energy-transfer assays and a nanothermometer, J. Phys. Chem. Lett. 6 (2015) 1293–1298, https://doi.org/10.1021/acs.jpclett.5b00378.
[97] M. Lettieri, P. Palladino, S. Scarano, M. Minunni, Protein-templated copper nanoclusters for fluorimetric determination of human serum albumin, Mikrochim. Acta 188 (2021) 116, https://doi.org/10.1007/s00604-021-04764-7.
[98] C. Wang, S. Shu, Y. Yao, Q. Song, A fluorescent biosensor of lysozyme-stabilized copper nanoclusters for the selective detection of glucose, RSC Adv. 5 (2015) 101599–101606, https://doi.org/10.1039/c5ra19421k.
[99] R. Ghosh, A.K. Sahoo, S.S. Ghosh, A. Paul, A. Chattopadhyay, Blue-emitting copper nanoclusters synthesized in the presence of lysozyme as candidates for cell labeling, ACS Appl. Mater. Interfaces 6 (2014) 3822–3828, https://doi.org/10.1021/am500040t.
[100] X. Li, X. Wu, F. Zhang, B. Zhao, Y. Li, Label-free detection of folic acid using a sensitive fluorescent probe based on ovalbumin stabilized copper nanoclusters, Talanta 195 (2019) 372–380, https://doi.org/10.1016/j.talanta.2018.11.067.
[101] H. Miao, D. Zhong, Z. Zhou, X. Yang, Papain-templated Cu nanoclusters: assaying and exhibiting dramatic antibacterial activity cooperating with H_2O_2, Nanoscale 7 (2015) 19066–19072, https://doi.org/10.1039/c5nr05362e.
[102] Q. Tan, J. Qiao, R. Zhang, L. Qi, Copper nanoclusters-modified with papaya juice for fluorescence turn-on detection of serum L-histidine today four files of proofs was sent to m.saksena@elsevier.com Please check the files, Microchem. J. 153 (2020) 2–7, https://doi.org/10.1016/j.microc.2019.104333.
[103] T. Zhao, X.W. He, W.Y. Li, Y.K. Zhang, Transferrin-directed preparation of red-emitting copper nanoclusters for targeted imaging of transferrin receptor over-expressed cancer cells, J. Mater. Chem. B 3 (2015) 2388–2394, https://doi.org/10.1039/c4tb02130d.
[104] T. Tang, J. Ouyang, L. Hu, L. Guo, M. Yang, X. Chen, Synthesis of peptide templated copper nanoclusters for fluorometric determination of Fe(III) in human serum, Microchim. Acta 183 (2016) 2831–2836, https://doi.org/10.1007/s00604-016-1935-z.
[105] Y. Wang, Y. Cui, R. Liu, Y. Wei, X. Jiang, H. Zhu, L. Gao, Y. Zhao, Z. Chai, X. Gao, Blue two-photon fluorescence metal cluster probe precisely marking cell nuclei of two cell lines, Chem. Commun. 49 (2013) 10724–10726, https://doi.org/10.1039/c3cc46690f.
[106] B. Rodrigues, P. Shende, Monodispersed metal-based dendrimeric nanoclusters for potentiation of anti-tuberculosis action, J. Mol. Liq. 304 (2020), 112731, https://doi.org/10.1016/j.molliq.2020.112731.
[107] T. Li, Z. Wang, D. Jiang, H. Wang, W.F. Lai, Y. Lv, Y. Zhai, A FRET biosensor based on MnO_2 nanosphere/copper nanocluster complex: from photoluminescence quenching to recovery and magnification, Sens. Actuators B Chem. 290 (2019) 535–543, https://doi.org/10.1016/j.snb.2019.04.033.
[108] J. Feng, Y. Ju, J. Liu, H. Zhang, X. Chen, Polyethyleneimine-templated copper nanoclusters via ascorbic acid reduction approach as ferric ion sensor, Anal. Chim. Acta 854 (2015) 153–160, https://doi.org/10.1016/j.aca.2014.11.024.
[109] Z. Wang, Y. Xiong, S.V. Kershaw, B. Chen, X. Yang, N. Goswami, W.F. Lai, J. Xie, A.L. Rogach, *In situ* fabrication of flexible, thermally stable, large-area, strongly luminescent copper nanocluster/polymer composite films, Chem. Mater. 29 (2017) 10206–10211, https://doi.org/10.1021/acs.chemmater.7b04239.
[110] S. Gou, Y.E. Shi, P. Li, H. Wang, T. Li, X. Zhuang, W. Li, Z. Wang, Stimuli-responsive luminescent copper nanoclusters in alginate and their sensing ability for glucose, ACS Appl. Mater. Interfaces (2019), https://doi.org/10.1021/acsami.8b20835.
[111] R. Patel, S. Bothra, R. Kumar, G. Crisponi, S.K. Sahoo, Pyridoxamine driven selective turn-off detection of picric acid using glutathione stabilized fluorescent copper nanoclusters and its applications with chemically modified cellulose strips, Biosens. Bioelectron. 102 (2018) 196–203, https://doi.org/10.1016/j.bios.2017.11.031.
[112] A. Dutta, U. Goswami, A. Chattopadhyay, Probing cancer cells through intracellular aggregation-induced emission kinetic rate of copper nanoclusters, ACS Appl. Mater. Interfaces 10 (2018) 19459–19472, https://doi.org/10.1021/acsami.8b05160.
[113] Y. Nerthigan, A.K. Sharma, S. Pandey, H.F. Wu, Cysteine capped copper/molybdenum bimetallic nanoclusters for fluorometric determination of methotrexate via the inner filter effect, Microchim. Acta (2019) 186, https://doi.org/10.1007/s00604-019-3230-2.
[114] H.B. Wang, B.B. Tao, N.N. Wu, H.D. Zhang, Y.M. Liu, Glutathione-stabilized copper nanoclusters mediated-inner filter effect for sensitive and selective determination of p-nitrophenol and alkaline phosphatase activity, Spectrochim. Acta Part A Mol. Biomol. Spectrosc. 271 (2022), 120948, https://doi.org/10.1016/j.saa.2022.120948.
[115] Y. Huang, H. Feng, W. Liu, S. Zhang, C. Tang, J. Chen, Z. Qian, Cation-driven luminescent self-assembled dots of copper nanoclusters with aggregation-induced emission for β-galactosidase activity monitoring, J. Mater. Chem. B 5 (2017) 5120–5127, https://doi.org/10.1039/c7tb00901a.
[116] R. Jalili, A. Khataee, Aluminum(III) triggered aggregation-induced emission of glutathione-capped copper nanoclusters as a fluorescent probe for creatinine, Microchim. Acta (2019) 186, https://doi.org/10.1007/s00604-018-3111-0.
[117] Y. Wang, T. Chen, Z. Zhang, Y. Ni, Cytidine-stabilized copper nanoclusters as a fluorescent probe for sensing of copper ions and hemin, RSC Adv. 8 (2018) 9057–9062, https://doi.org/10.1039/c7ra11383h.
[118] Z. Li, S. Guo, C. Lu, A highly selective fluorescent probe for sulfide ions based on aggregation of Cu nanocluster induced emission enhancement, Analyst 140 (2015) 2719–2725, https://doi.org/10.1039/c5an00017c.
[119] Y. Hu, Y. He, Y. Han, Y. Ge, G. Song, J. Zhou, Determination of the activity of alkaline phosphatase based on aggregation-induced quenching of the fluorescence of copper nanoclusters, Microchim. Acta (2019) 186, https://doi.org/10.1007/s00604-018-3122-x.
[120] Y.S. Borghei, M. Hosseini, M. Khoobi, M.R. Ganjali, Novel fluorometric assay for detection of cysteine as a reducing agent and template in formation of copper nanoclusters, J. Fluoresc. 27 (2017) 529–536, https://doi.org/10.1007/s10895-016-1980-3.

[121] H.B. Wang, B.B. Tao, A.L. Mao, Z.L. Xiao, Y.M. Liu, Self-assembled copper nanoclusters structure-dependent fluorescent enhancement for sensitive determination of tetracyclines by the restriction intramolecular motion, Sens. Actuators B Chem. 348 (2021), 130729, https://doi.org/10.1016/j.snb.2021.130729.
[122] L. Farzin, M. Shamsipur, L. Samandari, S. Sheibani, HIV biosensors for early diagnosis of infection: the intertwine of nanotechnology with sensing strategies, Talanta 206 (2020), 120201, https://doi.org/10.1016/j.talanta.2019.120201.
[123] J. Li, S. Zhang, Y. Yu, Y. Wang, L. Zhang, B. Lin, M. Guo, Y. Cao, A novel universal nanoplatform for ratiometric fluorescence biosensing based on silver nanoclusters beacon, Chem. Eng. J. (2019), 123526, https://doi.org/10.1016/j.cej.2019.123526.
[124] Y. Zhang, C. Zhang, C. Xu, X. Wang, C. Liu, G.I.N. Waterhouse, Y. Wang, H. Yin, Ultrasmall Au nanoclusters for biomedical and biosensing applications: a mini-review, Talanta 200 (2019) 432–442, https://doi.org/10.1016/j.talanta.2019.03.068.
[125] Y. Liu, P. Dong, Q. Jiang, F. Wang, D.W. Pang, X. Liu, Assembly-enhanced fluorescence from metal nanoclusters and quantum dots for highly sensitive biosensing, Sens. Actuators B Chem. 279 (2019) 334–341, https://doi.org/10.1016/j.snb.2018.10.016.
[126] Z. Liu, X. Jing, S. Zhang, Y. Tian, A copper nanocluster-based fluorescent probe for real-time imaging and ratiometric biosensing of calcium ions in neurons, Anal. Chem. 91 (2019) 2488–2497, https://doi.org/10.1021/acs.analchem.8b05360.
[127] L.C. Brazaca, L. Ribovski, B.C. Janegitz, V. Zucolotto, Nanostructured materials and nanoparticles for point of care (POC) medical biosensors, Med. Biosens. Point Care Appl. (2017) 229–254, https://doi.org/10.1016/B978-0-08-100072-4.00010-1.
[128] D. Quesada-González, A. Merkoçi, Nanomaterial-based devices for point-of-care diagnostic applications, Chem. Soc. Rev. 47 (2018) 4697–4709, https://doi.org/10.1039/c7cs00837f.
[129] L. Bezinge, A. Suea-Ngam, A.J. Demello, C.J. Shih, Nanomaterials for molecular signal amplification in electrochemical nucleic acid biosensing: recent advances and future prospects for point-of-care diagnostics, Mol. Syst. Des. Eng. 5 (2020) 49–66, https://doi.org/10.1039/c9me00135b.
[130] V. Baldoneschi, P. Palladino, S. Scarano, M. Minunni, Polynorepinephrine: state-of-the-art and perspective applications in biosensing and molecular recognition, Anal. Bioanal. Chem. (2020) 5945–5954, https://doi.org/10.1007/s00216-020-02578-9.
[131] F. Torrini, P. Palladino, A. Brittoli, V. Baldoneschi, M. Minunni, S. Scarano, Characterization of troponin T binding aptamers for an innovative enzyme-linked oligonucleotide assay (ELONA), Anal. Bioanal. Chem. 411 (2019) 7709–7716, https://doi.org/10.1007/s00216-019-02014-7.
[132] P. Palladino, A. Brittoli, E. Pascale, M. Minunni, S. Scarano, Colorimetric determination of total protein content in serum based on the polydopamine/protein adsorption competition on microplates, Talanta 198 (2019) 15–22, https://doi.org/10.1016/j.talanta.2019.01.095.
[133] R. Liu, C. Wang, J. Hu, Y. Su, Y. Lv, DNA-templated copper nanoparticles: versatile platform for label-free bioassays, TrAC Trends Anal. Chem. 105 (2018) 436–452, https://doi.org/10.1016/j.trac.2018.06.003.
[134] X.P. Wang, B.C. Yin, B.C. Ye, A novel fluorescence probe of dsDNA-templated copper nanoclusters for quantitative detection of microRNAs, RSC Adv. 3 (2013) 8633–8636, https://doi.org/10.1039/c3ra23296d.
[135] Y. Li, D. Tang, L. Zhu, J. Cai, C. Chu, J. Wang, M. Xia, Z. Cao, H. Zhu, Label-free detection of miRNA cancer markers based on terminal deoxynucleotidyl transferase-induced copper nanoclusters, Anal. Biochem. 585 (2019), 113346, https://doi.org/10.1016/j.ab.2019.113346.
[136] Y.S. Borghei, M. Hosseini, M.R. Ganjali, S. Hosseinkhani, Label-free fluorescent detection of microRNA-155 based on synthesis of hairpin DNA-templated copper nanoclusters by etching (top-down approach), Sens. Actuators B Chem. 248 (2017) 133–139, https://doi.org/10.1016/j.snb.2017.03.148.
[137] K.M. Koo, L.G. Carrascosa, M. Trau, DNA-directed assembly of copper nanoblocks with inbuilt fluorescent and electrochemical properties: application in simultaneous amplification-free analysis of multiple RNA species, Nano Res. 11 (2018) 940–952, https://doi.org/10.1007/s12274-017-1706-0.
[138] X. Jia, J. Li, L. Han, J. Ren, X. Yang, E. Wang, DNA-hosted copper nanoclusters for fluorescent identification of single nucleotide polymorphisms, ACS Nano 6 (2012) 3311–3317, https://doi.org/10.1021/nn3002455.
[139] C. Chen, C. Wang, H. Kou, S. Wu, Molecular inversion probe-rolling circle amplification with single-strand poly-T luminescent copper nanoclusters for fluorescent detection of single-nucleotide variant of SMN gene in diagnosis of spinal muscular atrophy, Anal. Chim. Acta (2020), https://doi.org/10.1016/j.aca.2020.04.026.
[140] S. Singh, M.K. Singh, P. Das, Biosensing of solitary and clustered abasic site DNA damage lesions with copper nanoclusters and carbon dots, Sens. Actuators B Chem. 255 (2018) 763–774, https://doi.org/10.1016/j.snb.2017.08.100.
[141] Y. Wang, T. Chen, Q. Zhuang, Y. Ni, One-pot aqueous synthesis of nucleoside-templated fluorescent copper nanoclusters and their application for discrimination of nucleosides, ACS Appl. Mater. Interfaces 9 (2017) 32135–32141, https://doi.org/10.1021/acsami.7b09768.
[142] T. Qing, C. Long, X. Wang, K. Zhang, P. Zhang, B. Feng, Detection of micrococcal nuclease for identifying Staphylococcus aureus based on DNA templated fluorescent copper nanoclusters, Microchim. Acta (2019) 186, https://doi.org/10.1007/s00604-019-3363-3.
[143] G. Liu, W. He, C. Liu, Sensitive detection of uracil-DNA glycosylase (UDG) activity based on terminal deoxynucleotidyl transferase-assisted formation of fluorescent copper nanoclusters (CuNCs), Talanta 195 (2019) 320–326, https://doi.org/10.1016/j.talanta.2018.11.083.
[144] Y. Ling, J. Zhou, X.F. Zhang, X.H. Wang, N.B. Li, H.Q. Luo, A ratiometric fluorescent sensor for sensitive detection of UDG using poly(thymine)-templated copper nanoclusters and DAPI with exonuclease III assisted amplification, Sens. Actuators B Chem. 286 (2019) 46–51, https://doi.org/10.1016/j.snb.2019.01.108.
[145] M. Cao, Y. Jin, B. Li, Simple and sensitive detection of uracil-DNA glycosylase activity using dsDNA-templated copper nanoclusters as fluorescent probes, Anal. Methods 8 (2016) 4319–4323, https://doi.org/10.1039/c6ay00900j.
[146] D. Gao, H. Zhang, Y. Xu, Y. Liu, H. Xu, J. Cui, Fluorescent copper nanoclusters as a nano-dye for DNA methyltransferase activity analysis and inhibitor screening, Anal. Biochem. 559 (2018) 5–10, https://doi.org/10.1016/j.ab.2018.08.011.
[147] F. Zhou, X. Cui, A. Shang, J. Lian, L. Yang, Y. Jin, B. Li, Fluorometric determination of the activity and inhibition of terminal deoxynucleotidyl transferase via *in-situ* formation of copper nanoclusters using enzymatically generated DNA as template, Microchim. Acta 184 (2017) 773–779, https://doi.org/10.1007/s00604-016-2065-3.
[148] H. Zhang, Y. Guan, X. Li, L. Lian, X. Wang, W. Gao, B. Zhu, X. Liu, D. Lou, Ultrasensitive biosensor for detection of mercury(II) ions based on DNA-Cu nanoclusters and exonuclease III-assisted signal amplification, Anal. Sci. 34 (2018) 1155–1161, https://doi.org/10.2116/analsci.18P124.
[149] Z. Gu, Z. Cao, Molecular switch-modulated fluorescent copper nanoclusters for selective and sensitive detection of histidine and cysteine, Anal. Bioanal. Chem. 410 (2018) 4991–4999, https://doi.org/10.1007/s00216-018-1149-9.
[150] H. Li, J. Chang, T. Hou, L. Ge, F. Li, A facile, sensitive, and highly specific trinitrophenol assay based on target-induced synergetic effects of acid induction and electron transfer towards DNA-templated copper nanoclusters, Talanta 160 (2016) 475–480, https://doi.org/10.1016/j.talanta.2016.07.030.
[151] C. Ma, M. Chen, H. Liu, K. Wu, H. He, K. Wang, A rapid method for the detection of humic acid based on the poly(thymine)-templated copper nanoparticles, Chin. Chem. Lett. 29 (2018) 136–138, https://doi.org/10.1016/j.cclet.2017.09.012.
[152] H.B. Wang, Y. Li, H.Y. Bai, Y.M. Liu, Fluorescent determination of dopamine using polythymine-templated copper nanoclusters, Anal. Lett. 51 (2018) 2868–2877, https://doi.org/10.1080/00032719.2018.1454457.
[153] X. Wang, C. Long, Z. Jiang, T. Qing, K. Zhang, P. Zhang, B. Feng, *In situ* synthesis of fluorescent copper nanoclusters for rapid detection of ascorbic acid in biological samples, Anal. Methods 11 (2019) 4580–4585, https://doi.org/10.1039/c9ay01627a.
[154] Y. Xiong, B. Gao, K. Wu, Y. Wu, Y. Chai, X. Huang, Y. Xiong, Fluorescence immunoassay based on the enzyme cleaving ss-DNA to regulate the synthesis of histone-ds-poly(AT) templated copper nanoparticles, Nanoscale 10 (2018) 19890–19897, https://doi.org/10.1039/c8nr06175k.
[155] X. Zhang, Q. Liu, Y. Jin, B. Li, Determination of the activity of T4 polynucleotide kinase phosphatase by exploiting the sequence-dependent fluorescence of DNA-templated copper nanoclusters, Microchim. Acta 186 (2019) 1–9, https://doi.org/10.1007/s00604-018-3102-1.
[156] Y. Hu, Q. Zhang, L. Xu, J. Wang, J. Rao, Z. Guo, S. Wang, Signal-on electrochemical assay for label-free detection of TdT and BamHI activity based on grown DNA nanowire-templated copper nanoclusters, Anal. Bioanal. Chem. 409 (2017) 6677–6688, https://doi.org/10.1007/s00216-017-0623-0.
[157] H. Liao, Y. Zhou, Y. Chai, R. Yuan, An ultrasensitive electrochemiluminescence biosensor for detection of MicroRNA by *in-situ* electrochemically generated copper nanoclusters as luminophore and TiO_2 as coreaction accelerator, Biosens. Bioelectron. 114 (2018) 10–14, https://doi.org/10.1016/j.bios.2018.05.011.
[158] Y. Zhou, H. Wang, H. Zhang, Y. Chai, R. Yuan, Programmable modulation of copper nanoclusters electrochemiluminescence via DNA nanocranes for ultrasensitive detection of microRNA, Anal. Chem. 90 (2018) 3543–3549, https://doi.org/10.1021/acs.analchem.7b05402.
[159] Y.S. Borghei, M. Hosseini, M.R. Ganjali, Visual detection of miRNA using peroxidase-like catalytic activity of DNA-CuNCs and methylene blue as indicator, Clin. Chim. Acta 483 (2018) 119–125, https://doi.org/10.1016/j.cca.2018.04.031.
[160] X. Mao, S. Liu, C. Yang, F. Liu, K. Wang, G. Chen, Colorimetric detection of hepatitis B virus (HBV) DNA based on DNA-templated copper nanoclusters, Anal. Chim. Acta 909 (2016) 101–108, https://doi.org/10.1016/j.aca.2016.01.009.
[161] M. Chen, Z. Ning, K. Chen, Y. Zhang, Y. Shen, Recent advances of electrochemiluminescent system in bioassay, J. Anal. Test. 4 (2020) 57–75, https://doi.org/10.1007/s41664-020-00136-x.
[162] R.S. Aparna, J.S. Anjali Devi, P. Sachidanandan, S. George, Polyethylene imine capped copper nanoclusters- fluorescent and colorimetric onsite sensor for the trace level detection of TNT, Sens. Actuators B Chem. 254 (2018) 811–819, https://doi.org/10.1016/j.snb.2017.07.097.
[163] P.X. Yuan, S.Y. Deng, C.Y. Zheng, S. Cosnier, D. Shan, *In situ* formed copper nanoparticles templated by TdT-mediated DNA for enhanced SPR sensor-based DNA assay, Biosens. Bioelectron. 97 (2017) 1–7, https://doi.org/10.1016/j.bios.2017.05.033.
[164] C.G. Pheeney, J.K. Barton, DNA electrochemistry with tethered methylene blue, Langmuir 28 (2012) 7063–7070, https://doi.org/10.1021/la300566x.
[165] S. Mariani, S. Scarano, J. Spadavecchia, M. Minunni, A reusable optical biosensor for the ultrasensitive and selective detection of unamplified human genomic DNA with gold nanostars, Biosens. Bioelectron. 74 (2015) 981–988, https://doi.org/10.1016/j.bios.2015.07.071.
[166] S. Mariani, S. Scarano, M.L. Ermini, M. Bonini, M. Minunni, Investigating nanoparticle properties in plasmonic nanoarchitectures with DNA by surface

plasmon resonance imaging, Chem. Commun. 51 (2015) 6587–6590, https://doi.org/10.1039/c4cc09889g.
[167] M. Calcagno, R. D'Agata, G. Breveglieri, M. Borgatti, N. Bellassai, R. Gambari, G. Spoto, Nanoparticle-enhanced surface plasmon resonance imaging enables the ultrasensitive detection of non-amplified cell-free fetal DNA for non-invasive prenatal testing, Anal. Chem. 94 (2022) 1118–1125, https://doi.org/10.1021/acs.analchem.1c04196.
[168] C. Lee, J. Gang, Label-free rapid and simple detection of exonuclease III activity with DNA-templated copper nanoclusters, J. Microbiol. Biotechnol. 28 (2018) 1467–1472.
[169] Y. Seok Kim, N.H. Ahmad Raston, M. Bock Gu, Aptamer-based nanobiosensors, Biosens. Bioelectron. 76 (2016) 2–19, https://doi.org/10.1016/j.bios.2015.06.040.
[170] B. Zhang, C. Wei, The sensitive detection of ATP and ADA based on turn-on fluorescent copper/silver nanoclusters, Anal. Bioanal. Chem. (2020) 2529–2536, https://doi.org/10.1007/s00216-020-02476-0.
[171] Y.M. Wang, J.W. Liu, L.Y. Duan, S.J. Liu, J.H. Jiang, Aptamer-based fluorometric determination of ATP by using target-cycling strand displacement amplification and copper nanoclusters, Microchim. Acta 184 (2017) 4183–4188, https://doi.org/10.1007/s00604-017-2337-6.
[172] M. Wang, S. Wang, D. Su, X. Su, Copper nanoclusters/polydopamine nanospheres based fluorescence aptasensor for protein kinase activity determination, Anal. Chim. Acta 1035 (2018) 184–191, https://doi.org/10.1016/j.aca.2018.06.043.
[173] H.Y. Dar, Y. Lone, R.K. Koiri, P.K. Mishra, R.K. Srivastava, Microcystin-leucine arginine (MC-LR) induces bone loss and impairs bone micro-architecture by modulating host immunity in mice: implications for bone health, Environ. Pollut. 238 (2018) 792–802, https://doi.org/10.1016/J.ENVPOL.2018.03.059.
[174] Y. Zhang, Z. Zhu, X. Teng, Y. Lai, S. Pu, P. Pang, H. Wang, C. Yang, C.J. Barrow, W. Yang, Enzyme-free fluorescent detection of microcystin-LR using hairpin DNA-templated copper nanoclusters as signal indicator, Talanta 202 (2019) 279–284, https://doi.org/10.1016/j.talanta.2019.05.013.
[175] F.M. Moghadam, M. Rahaie, A signal-on nanobiosensor for VEGF 165 detection based on supraparticle copper nanoclusters formed on bivalent aptamer, Biosens. Bioelectron. 132 (2019) 186–195, https://doi.org/10.1016/j.bios.2019.02.046.
[176] Y. Wang, X. Zhang, L. Zhao, T. Bao, W. Wen, X. Zhang, S. Wang, Integrated amplified aptasensor with *in-situ* precise preparation of copper nanoclusters for ultrasensitive electrochemical detection of microRNA 21, Biosens. Bioelectron. 98 (2017) 386–391, https://doi.org/10.1016/j.bios.2017.07.009.
[177] M. Wang, Z. Lin, Q. Liu, S. Jiang, H. Liu, X. Su, DNA-hosted copper nanoclusters/graphene oxide based fluorescent biosensor for protein kinase activity detection, Anal. Chim. Acta 1012 (2018) 66–73, https://doi.org/10.1016/j.aca.2018.01.029.
[178] A.D. Kurdekar, C. Sai Manohar, L.A.A. Chunduri, M.K. Haleyurgirisetty, I. K. Hewlett, V. Kamisetti, Computational design and clinical demonstration of a copper nanocluster based universal immunosensor for sensitive diagnostics, Nanoscale Adv. 2 (2020) 304–314, https://doi.org/10.1039/c9na00503j.
[179] L. Zhao, Z. Ma, New immunoprobes based on bovine serum albumin-stabilized copper nanoclusters with triple signal amplification for ultrasensitive electrochemical immunosensing for tumor marker, Sens. Actuators B Chem. 241 (2017) 849–854, https://doi.org/10.1016/j.snb.2016.11.012.
[180] Y. Chen, S. Zhang, H. Dai, Z. Hong, Y. Lin, A multiple mixed TiO_2 mesocrystal junction based PEC-colorimetric immunoassay for specific recognition of lipolysis stimulated lipoprotein receptor, Biosens. Bioelectron. 148 (2020), 111809, https://doi.org/10.1016/j.bios.2019.111809.
[181] R. Li, Q. Liu, Y. Jin, B. Li, Fluorescent enzyme-linked immunoassay strategy based on enzyme-triggered *in-situ* synthesis of fluorescent copper nanoclusters, Sens. Actuators B Chem. 281 (2019) 28–33, https://doi.org/10.1016/j.snb.2018.09.128.
[182] S. Lv, Y. Li, K. Zhang, Z. Lin, D. Tang, Carbon Dots/g-C3N4 nanoheterostructures-based signal-generation tags for photoelectrochemical immunoassay of cancer biomarkers coupling with copper nanoclusters, ACS Appl. Mater. Interfaces 9 (2017) 38336–38343, https://doi.org/10.1021/acsami.7b13272.
[183] L.P. Mei, X.Y. Jiang, X.D. Yu, Z. Wei-Wei, J.J. Xu, C. Hong-Yuan, Cu nanoclusters-encapsulated liposomes : toward sensitive liposomal photoelectrochemical immunoassay, Anal. Chem. 90 (2018) 2749–2755, https://doi.org/10.1021/acs.analchem.7b04789.
[184] W. Zhuang, Y. Li, J. Chen, W. Liu, H. Huang, Copper nanocluster-labeled hybridization chain reaction for potentiometric immunoassay of matrix metalloproteinase-7 in acute kidney injury and renal cancer, Anal. Methods 11 (2019) 2597–2604, https://doi.org/10.1039/c9ay00681h.
[185] Y. Zhao, X. Wang, J. Mi, Y. Jiang, C. Wang, Metal nanoclusters–based ratiometric fluorescent probes from design to sensing applications, Part. Part. Syst. Charact. 36 (2019), 1900298, https://doi.org/10.1002/PPSC.201900298.
[186] S. Garima, S. Jindal, S. Garg, I. Matai, G. Packirisamy, A. Sachdev, Dual-emission copper nanoclusters–based ratiometric fluorescent probe for intracellular detection of hydroxyl and superoxide anion species, Microchim. Acta (2021) 188, https://doi.org/10.1007/s00604-020-04683-z.
[187] Y. Shi, W. Li, X. Feng, L. Lin, P. Nie, J. Shi, X. Zou, Y. He, Sensing of mercury ions in Porphyra by Copper @ Gold nanoclusters based ratiometric fluorescent aptasensor, Food Chem. 344 (2021), 128694, https://doi.org/10.1016/J.FOODCHEM.2020.128694.
[188] W. Li, X. Hu, Q. Li, Y. Shi, X. Zhai, Y. Xu, Z. Li, X. Huang, X. Wang, J. Shi, X. Zou, S. Kang, Copper nanoclusters @ nitrogen-doped carbon quantum dots-based ratiometric fluorescence probe for lead (II) ions detection in porphyra, Food Chem. 320 (2020), 126623, https://doi.org/10.1016/J.FOODCHEM.2020.126623.
[189] C. Ma, P. Li, L. Xia, F. Qu, R.M. Kong, Z.L. Song, A novel ratiometric fluorescence nanoprobe for sensitive determination of uric acid based on CD@ZIF-CuNC nanocomposites, Microchim. Acta (2021) 188, https://doi.org/10.1007/s00604-021-04914-x.
[190] S.H. Park, N. Kwon, J.H. Lee, J. Yoon, I. Shin, Synthetic ratiometric fluorescent probes for detection of ions, Chem. Soc. Rev. 49 (2020) 143–179, https://doi.org/10.1039/C9CS00243J.
[191] X. Hu, H. Cao, W. Dong, J. Tang, Ratiometric fluorescent sensing of ethanol based on copper nanoclusters with tunable dual emission, Talanta 233 (2021), 122480, https://doi.org/10.1016/J.TALANTA.2021.122480.
[192] B.B. Tao, N.N. Wu, H.D. Zhang, H.B. Wang, Blocking the Cu (II) ions mediated catalytical ability for construction of ratiometric fluorescence sensing platform based on glutathione-stabilized copper nanoclusters, J. Electrochem. Soc. 169 (2022), 037529, https://doi.org/10.1149/1945-7111/AC5F1E.
[193] P.S. Zangabad, S. Mirkiani, S. Shahsavari, B. Masoudi, M. Masroor, H. Hamed, Z. Jafari, Y.D. Taghipour, H. Hashemi, M. Karimi, M.R. Hamblin, Stimulus-responsive liposomes as smart nanoplatforms for drug delivery applications, Nanotechnol. Rev. 7 (2018) 95–122, https://doi.org/10.1515/ntrev-2017-0154.
[194] M. Karimi, P. Sahandi Zangabad, A. Ghasemi, M. Amiri, M. Bahrami, H. Malekzad, H. Ghahramanzadeh Asl, Z. Mahdieh, M. Bozorgomid, A. Ghasemi, M.R. Rahmani Taji Boyuk, M.R. Hamblin, Temperature-responsive smart nanocarriers for delivery of therapeutic agents: applications and recent advances, ACS Appl. Mater. Interfaces 8 (2016) 21107–21133, https://doi.org/10.1021/acsami.6b00371.
[195] S. Shahsavari, Cellular functions analyses based on nanorobotics, J. Nanomedicine Res. 5 (2017) 34–35, https://doi.org/10.15406/jnmr.2017.05.00101.
[196] H. Cao, Z. Chen, H. Zheng, Y. Huang, Copper nanoclusters as a highly sensitive and selective fluorescence sensor for ferric ions in serum and living cells by imaging, Biosens. Bioelectron. 62 (2014) 189–195, https://doi.org/10.1016/j.bios.2014.06.049.
[197] N.K. Das, S. Ghosh, A. Priya, S. Datta, S. Mukherjee, Luminescent copper nanoclusters as a specific cell-imaging probe and a selective metal ion sensor, J. Phys. Chem. C 119 (2015) 24657–24664, https://doi.org/10.1021/acs.jpcc.5b08123.
[198] R. Ghosh, U. Goswami, S.S. Ghosh, A. Paul, A. Chattopadhyay, Synergistic anticancer activity of fluorescent copper nanoclusters and cisplatin delivered through a hydrogel nanocarrier, ACS Appl. Mater. Interfaces 7 (2015) 209–222, https://doi.org/10.1021/am505799q.
[199] X. Zhu, H. Shi, Y. Shen, B. Zhang, J. Zhao, G. Li, A green method of staining DNA in polyacrylamide gel electrophoresis based on fluorescent copper nanoclusters synthesized *in situ*, Nano Res. 8 (2015) 2714–2720, https://doi.org/10.1007/s12274-015-0778-y.
[200] Z. Wang, C.C. Zhang, J. Gao, Q. Wang, Copper clusters-based luminescence assay for tetracycline and cellular imaging studies, J. Lumin. 190 (2017) 115–122, https://doi.org/10.1016/j.jlumin.2017.05.038.
[201] A. Baghdasaryan, R. Grillo, S.R. Bhattacharya, M. Sharma, E. Reginato, H. Theraulaz, I. Dolamic, M. Dadras, S. Rudaz, E. Varesio, T. Burgi, Facile synthesis, size-separation, characterization, and antimicrobial properties of thiolated copper clusters, ACS Appl. Nano Mater. 1 (2018) 4258–4267, https://doi.org/10.1021/acsanm.8b01049.